NRC·CNRC

NRC Publications Archive
Archives des publications du CNRC

Validation of SkyVision

Laouadi, A.; Arsenault, C. D.

For the publisher's version, please access the DOI link below./ Pour consulter la version de l'éditeur, utilisez le lien DOI ci-dessous.

Publisher's version / Version de l'éditeur:
https://doi.org/10.4224/20378038
Research Report (National Research Council of Canada. Institute for Research in Construction), 2004-06-01

NRC Publications Archive Record / Notice des Archives des publications du CNRC :
https://nrc-publications.canada.ca/eng/view/object/?id=4f1dca22-acba-4a8a-8045-75bb6ee6c7e5
https://publications-cnrc.canada.ca/fra/voir/objet/?id=4f1dca22-acba-4a8a-8045-75bb6ee6c7e5

Access and use of this website and the material on it are subject to the Terms and Conditions set forth at
https://nrc-publications.canada.ca/eng/copyright
READ THESE TERMS AND CONDITIONS CAREFULLY BEFORE USING THIS WEBSITE.

L'accès à ce site Web et l'utilisation de son contenu sont assujettis aux conditions présentées dans le site
https://publications-cnrc.canada.ca/fra/droits
LISEZ CES CONDITIONS ATTENTIVEMENT AVANT D'UTILISER CE SITE WEB.

Questions? Contact the NRC Publications Archive team at PublicationsArchive-ArchivesPublications@nrc-cnrc.gc.ca. If you wish to email the authors directly, please see the first page of the publication for their contact information.

Vous avez des questions? Nous pouvons vous aider. Pour communiquer directement avec un auteur, consultez la première page de la revue dans laquelle son article a été publié afin de trouver ses coordonnées. Si vous n'arrivez pas à les repérer, communiquez avec nous à PublicationsArchive-ArchivesPublications@nrc-cnrc.gc.ca.

National Research Council Canada | Conseil national de recherches Canada

Canada

National Research Council Canada
Conseil national de recherches Canada

NRC · CNRC

Validation of SkyVision

Laouadi, A.; Arsenault, C.

IRC-RR-167

June 2004

http://irc.nrc-cnrc.gc.ca/ircpubs

construction
Institute for Research in Construction
Institut de recherche en construction
IRC

VALIDATION OF SKYVISION

Abdelaziz Laouadi (Aziz) and Chantal Arsenault

Indoor Environment Research Program

Institute for Research in Construction

National Research Council Canada

1200 Montreal Road, Building M-24

Ottawa, Ontario K1A 0R6

Report No. IRC-RR-167

June 2004

TABLE OF CONTENTS

LIST OF FIGURES

LIST OF TABLES

EXECUTIVE SUMMARY

IRC has released the final version of its SkyVision software for predicting skylight performance after extensive validation testing on the beta version released last year. Skylight designers, skylight manufacturers, building designers, fenestration rating councils, architects and educators can use the tool to predict the daylighting performance and energy saving potential of conventional and tubular skylights. This report outlines the test methodology to measure the skylight performance, and presents the comparison study between the software's predictions and the actual measurements. This report also includes a comparison with the results of the California PIER (Public Interest Energy Research) program for the effective transmittance of skylight and well combinations. The results of the PIER program covered additional skylight settings, and provided valuable benchmarks not only for the effective transmittance, but also for the thermal transmittance (U-value) and the solar heat gain coefficient of projecting skylights.

A series of experiments were carried out to measure the skylight transmittance and indoor daylight illuminance under real sky conditions at the premises of the National Research Council of Canada, Ottawa, Ontario. A rectangular wooden box of 2.32 m (91.5") length x 1.73 m (68") width x 1.22 m (48") height was erected as a scale model of a simple commercial building. The top surface of the box was fitted with a curbed opening to accommodate the skylights to be tested. Seven skylight shapes were tested: two circular dome models, one with clear and one with white acrylic glazing; two rectangular bubble models, one with clear and one with white acrylic glazing; a clear acrylic hexagonal pyramid model; a clear polycarbonate barrel vault model; and a tubular skylight model. To measure the indoor daylight illuminance of the skylight, 16 illuminance sensors were used and uniformly spaced within the floor surface of the box. To measure the skylight transmittance, five illuminance sensors were placed at the top level of the curb (with the exception that the lightpipe used only one sensor). Each measurement required a special set-up to accurately characterize the skylight performance. For example, for the transmittance measurement, a black photographic fabric was dropped from the edges of the skylight to the floor surface of the box to avoid any significant reflected light back to the skylight surface. In addition, a rooftop weather station measured the outdoor diffuse and global solar radiation and illuminance. Data acquisition was done every minute, and averaged every five minutes. The measurements were taken for a whole day period, covering different sky conditions: overcast, partly cloudy and clear sunny skies.

When the software's predictions for the skylight transmittance were compared with the actual measurements, they compared very well, except for the hexagonal pyramidal skylight. The hexagonal pyramid surface exhibited some lens effect around the surface vertices. This effect caused some of the sensors to measure very low or very high illuminances (under sunny conditions the interior illuminance sensor readings were up to 50% more than the outside illuminance!). The surface lens effect was not

possible to model in SkyVision. As for the skylight indoor illuminance comparison, the software's predictions compared very well with the actual measurements for all occurrences of sky conditions.

In the comparison with the PIER results, the software's predictions of the effective transmittance of the skylight and well combinations compared well overall, particularly for the diffuse well combinations. The differences between the predictions and measurements were mainly attributed to the input parameters, which were not measured, and to the limitations of the current version of SkyVision, particularly in handling skylights with a mixture of clear and diffuse glazing, and skylights combined with a diffuse curb and specular well.

ACKNOWLDGEMENTS

This work was funded by the Institute for Research in Construction (IRC) of the National Research Council Canada; the CETC Buildings Group and Panel on Energy Research and Development (PERD) of the Natural Resources Canada; and the Public Works and Government Services Canada (PWGSC). In addition, a number of companies donated skylight products for testing, including: Artistic Skylight Domes Ltd. in Etobicoke, Ontario; Mac Plastics Ltd. in Edmonton, Alberta; and Energy Harmony in St. Catharines, Ontario. The authors were very thankful for their contribution. The authors would also like to extend their gratitude to Dr. Guy Newsham (Group leader at IRC/IE), Dr. Christoph Reinhart (IRC/IE), Rogers Marchand (IRC/IE), Ivan Pasini and Karen Pero (PWGSC), and Francois Dubrous (NRCan) for their continuous technical support and advice throughout the project, and to Jon McHugh (Heschong Mahone Group Inc., CA, USA) for providing the PIER results for comparison.

INTRODUCTION

The Institute for Research in Construction (IRC) of the National Research Council of Canada has completed a research project on the modeling and simulation of the daylighting performance and energy-saving potential of conventional and tubular skylights. The project has culminated in a free software tool called SkyVision. The energy benefits of skylights can be substantial, particularly in commercial buildings (McHugh et al. 2004). However, these energy benefits have not been fully exploited due to a number of theoretical and technical challenges. The lack of design tools is a major hurdle for building designers to adopt such products and quantify their energy benefits. For example, fenestration simulation software such as FRAMEplus5.1 (CANMET, 2003) and WINDOW5.1 (LBL, 2003a) deal with only planar and transparent geometry, such as windows and flat skylights. Sophisticated lighting simulation software such as RADIANCE (LBL, 2003b), LUMEN MICRO (Lighting Technologies, 2003) and SUPERLITE **(**IEA SHC Task 21, 2000**)**, are not only cumbersome to use, but they do not provide any output related to the skylight optical characteristics, which are useful for skylight product rating and selection. Specialized skylight software such as the SkyCalc program (HMG, 2003) is limited to some USA climate regions, and handles only flat translucent skylights.

SkyVision aims to assist skylight manufacturers and building designers in developing appropriate skylight designs for given building types and daylighting applications. SkyVision may also help fenestration rating councils to rate skylight products. SkyVision calculates the overall optical characteristics of conventional and tubular skylights, performance indicators of skylight/room interfaces, indoor daylight availability, and annual lighting energy savings. To maximize the energy-saving potential of skylights, SkyVision accounts for the skylight shape and glazing type, curb/well geometry, building location and orientation, lighting and shading controls, and prevailing climate. It is intended for use by skylight manufacturers, architects, engineers, fenestration councils, and research and educational institutions.

IRC released two beta versions in the previous year for testing and evaluation by the end-users. This was followed by extensive measurements and comparison studies to validate the software's predictions. The user's feedback and comparison studies were extremely useful to shape the final look of the software and fine-tune its predictions models. The final version of SkyVision is now available on the web (http://irc.nrc-cnrc.gc.ca/ie/light/skyvision/). More details on the software can also be found in the distribution web site.

OBJECTIVES

This report addresses the experimental validation of SkyVision. Extensive measurements of skylight performance under real sky conditions were carried out for this purpose. The measurements included the visible transmittance of the skylight and the indoor daylight illuminance. Other validation studies (model to model comparisons) are found in Laouadi et al. (2003a) and (2003b). The specific objectives of this report are:

- To outline the measurement methodology;
- To compare the software's predictions with the actual measurements; and
- To compare the software's predictions with the measurements from the California PIER program (McHugh et al. 2004).

MEASUREMENT METHODOLOGY

Projecting skylights exhibit different performance than planar fenestration (Laouadi and Atif 1998, 2002; McHugh et al. 2004). One of the most important parameters of skylights are their optical properties. Skylight optical properties are not only important for product rating but also for daylighting and energy performance predictions. Contrary to planar fenestration, there is no standard procedure to measure the skylight optical properties under laboratory or real settings. For example, the ASTM Standard E972-96 (or E1084-86/96) to measure the transmittance of flat sheets of glazing under sunlight cannot be used for projecting skylights for a number of reasons. One main reason is that the use of one illuminance sensor underneath the glazing is not adequate to calculate the transmitted energy through the skylight, especially for large skylight apertures. Furthermore, due to the forming process of skylight glazing, the skylight surface may exhibit a variable thickness, and therefore variable local transmittance (for example, some surface points may exhibit lens effects). This effect may result in the misrepresentation of the overall performance. In addition, skylights transmit radiation not only by direct transmission but also by inter-reflection within the surfaces inside the skylight. Capturing the inter-reflected energy needs some sensors placed close to the bottom surface of the skylight.

Recognizing this gap in skylight performance measurements, IRC adopted an experimental procedure to measure the skylight visible transmittance and skylight daylight illuminance under real sky conditions; details follow.

EXPERIMENTAL SETUP

A rectangular wooden box was erected as a scale model of a simple commercial building, and was placed on the roof of one of the buildings of the Institute for Research in Construction of the National Research Council of Canada. The building is located in Ottawa (latitude = 45.32^{o} north, and longitude = 75.67^{o} east), Ontario. The box measured 2.32 m (91.5") length x 1.73 m (68") width x 1.22 m (48") height, and was oriented towards the south-east with an angle of 28^{o} from the south cardinal direction. Figure 1 shows the box as placed on the building roof. The inside surfaces of the box were uniformly painted. The reflectance of the inside surface of a sample cut from box ceiling was measured at the Institute for National Measurement Standards of NRC, and was found to be 55%. The outside surface of the box was painted with a paint that looks like the surroundings (gravel) with an approximate reflectance of 25% (measured using a hand-held luminance meter). The top surface of the box was fitted with a

curbed opening to accommodate the skylights to be tested. The opening measured 1.28 m (50.5”) length x 0.92 m (36”) width. The curb was made of wood and measured 0.12 m (4.75”) in height. The curb inside surface was painted with the same paint as the box interior surfaces. Two small openings (6” x 6”) were made in the floor surface near the north border, and one in the middle top-portion of the south-facing wall to ventilate the inside space. The south-facing opening was equipped with an exhaust fan to evacuate any moist inside air and to avoid any possible space overheating that may affect the sensor readings. The outdoor and indoor space temperatures were monitored using thermocouple sensors.

Figure 1 Measurement box as placed on the roof of the building

SKYLIGHT ILLUMINANCE MEASUREMENT SETUP

To measure the average illuminance of the box floor surface, 16 illuminance sensors were used and uniformly spaced over the floor surface: one in the center, seven on an inner ring and eight on an outer ring near the walls. The illuminance sensors were spaced at intervals of one fifth (1/5) of the floor length or width distance. One additional illuminance sensor was placed on the roof of the box to measure the outdoor global (sky-diffuse and sun-beam) horizontal illuminance. Figure 2 shows a schematic description of the measurement setup and illuminance sensors positions on the floor surface.

The average floor illuminance was calculated based on the area proportion of each sensor as follows:

$$E_{floor} = \frac{E_{center} + 8/7 \cdot \sum_{i=1}^{7} E_{i,inner} + 2 \cdot \sum_{i=1}^{8} E_{i,outer}}{25} \quad (1)$$

where:

E_{floor} : average illuminance of the floor surface;

E_{center} : illuminance from the center sensor;

$E_{i,\ inner}$: illuminance from the i^{th} sensor of the inner ring; and

$E_{i,\ outer}$: illuminance from the i^{th} sensor of the outer ring.

SKYLIGHT VISIBLE TRANSMITTANCE MEASUREMENT SETUP

The skylight visible transmittance is defined as the ratio of the transmitted energy flux exiting from the skylight aperture opening to the flux incident on the horizontally projected skylight surface. In this regard, the effects of the curb or well spaces are not included in this definition.

To measure the transmitted energy flux, five illuminance sensors (except for the tubular skylight that used one sensor) were placed at the top level of the curb, one in the center and one on each side between the center and the edge of the skylight. The sensor spacing was chosen so that each sensor represented the same surface area. To avoid any significant reflected light back to the skylight surface, black fabric was dropped from the edges of the skylight to the floor surface of the box. The five sensors were placed on a black wooden support. Figure 3 shows a schematic description of the measurement setup and sensor positions.

The skylight visible transmittance was calculated as follows:

$$VT_m = \frac{\sum_{i=1}^{5} E_i / 5}{E_{glob}} \qquad (2)$$

where:

E_i : illuminance from the i^{th} sensor;

E_{glob} : outdoor global horizontal illuminance from the sky diffuse and sun beam lights; and

VT_m : measured skylight visible transmittance for the global light.

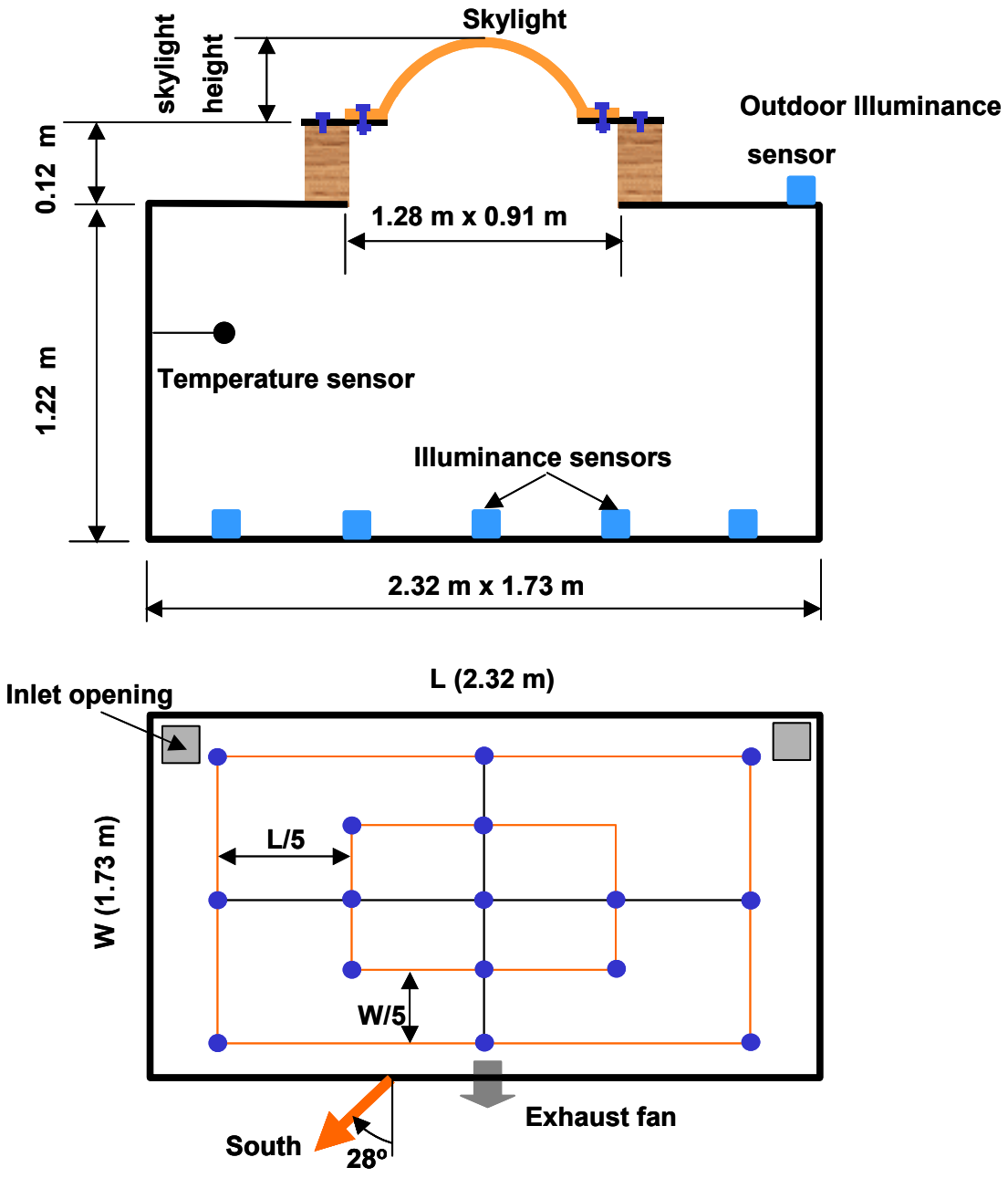

Figure 2 Schematic description of the skylight illuminance measurement setup (section above and plan below)

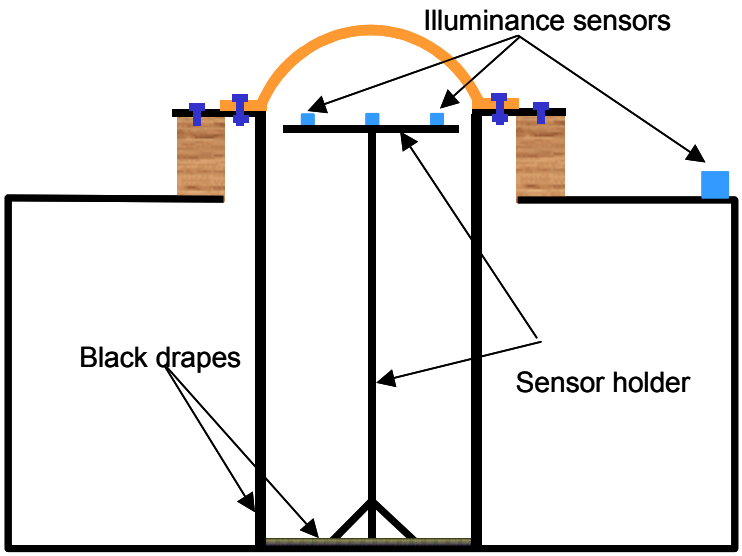

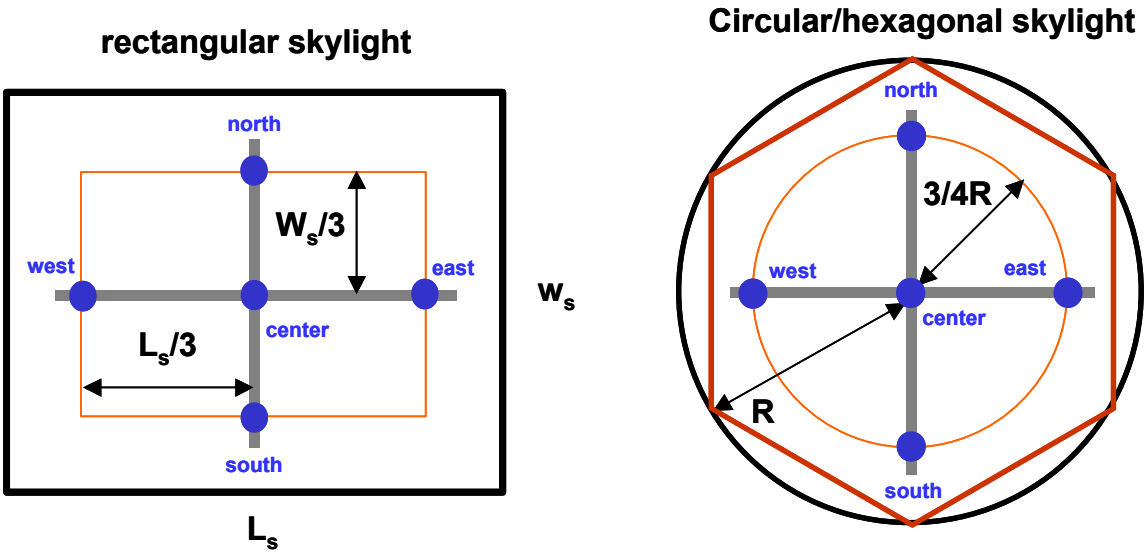

Figure 3 Schematic description of the skylight visible transmittance measurement setup (section above and plan below)

WEATHER STATION

The outdoor solar radiation and illuminance were measured at the rooftop permanent weather station using a YANKEE SDR-1 radiometer. The YANKEE had two sensors for the solar irradiance and illuminance measurement. An automatic controlled shadow band periodically passed over the sensors in order to measure the diffuse horizontal irradiance and illuminance. When the band was removed from the sensor, global horizontal irradiance and illuminance measurements were taken. Direct normal irradiance

and illuminance were automatically calculated from the diffuse and the global values measurements. The complete cycle took 15 seconds to switch from global to diffuse measurements. Figure 4 shows the rooftop weather station.

Figure 4 Solar radiation and illuminance weather station

MEASUREMENT EQUIPMENT AND CALIBRATION

The illuminance sensors were of type LI-COR model LI-210SA. The sensors were cosine corrected up to an incidence angle of 80^{o}, and had a sensitivity response function within 5% of the CIE $V\lambda$ photometric efficiency function. All the illuminance sensors were calibrated by the manufacturer and checked at the IRC's laboratory. The maximum calibration uncertainty was about 5% within the sensor sensitivity range (from an incidence angle of 0^{o} to 80^{o}; the error is very large beyond this angle). The YANKEE radiometer was calibrated by the manufacturer. The YANKEE calibration was also checked at IRC by comparing its readings with the outdoor LI-COR sensor. This sensor comparison is presented in figure 5 under a clear and sunny sky.

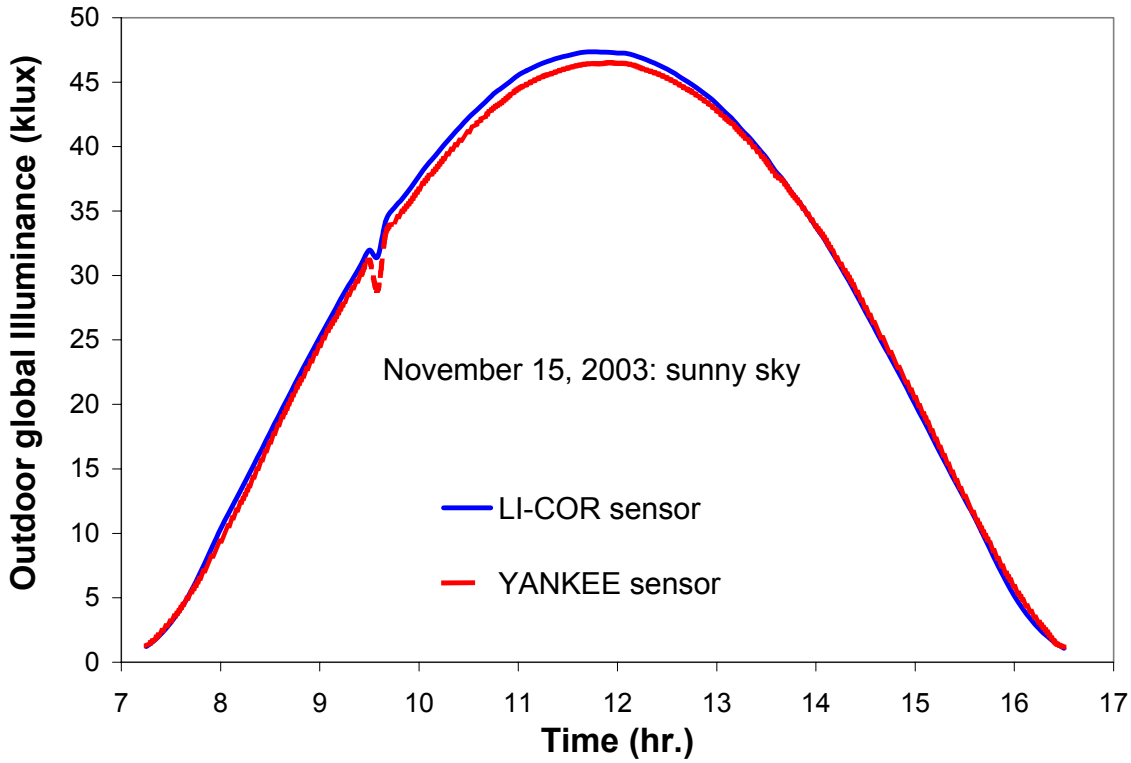

Figure 5 Comparison of the LI-COR and YANKEE illuminance sensor readings

TEST SPECIMEN

Seven skylight shapes were tested: (1) circular dome with single clear acrylic glazing, (2) circular dome with single white acrylic glazing, (3) hexagonal pyramid with single clear acrylic glazing, (4) rectangular bubble with single clear acrylic glazing, (5) rectangular bubble with single white acrylic glazing, (6) barrel vault with single clear polycarbonate glazing, and (7) tubular skylight. Table 1 summarizes the physical properties of the tested shapes. All the skylights were supplied by the manufacturers, except the barrel vault, which was made in-house. Figures 6 to 12 show the tested skylights as installed on the roof of the measurement box.

Table 1 Physical characteristics of the tested skylights. The optical properties of the glazing sheet the skylight was made of at a normal incidence angle were supplied by the manufacturer, unless otherwise stated.

Skylight Shape	Interior Dimensions	Material	Optical Properties (visible spectrum)
Clear circular dome	Diameter = 0.84 m (33”) Height = 0.2 m (8”)	6 mm clear acrylic	Transmittance = 0.92 Reflectance = 0.074[(1)]
White circular dome	Diameter = 0.84 m (33”) Height = 0.2 m (8”)	6 mm white acrylic #2447	Transmittance = 0.53 Reflectance = 0.10[(2)]
Clear hexagonal pyramid	Diameter = 0.84 m (33”) Height = 0.23 m (9”)	6 mm clear acrylic	Transmittance = 0.92 Reflectance = 0.074
Clear rectangular bubble	Length = 1.18 m (46.5”) Width = 0.57 m (22.5”) Height = 0.22 m (8.75”)	5 mm clear acrylic	Transmittance = 0.92 Reflectance = 0.074
White rectangular bubble	Length = 1.18 m (46.5”) Width = 0.57 m (22.5”) Height = 0.22 m (8.75”)	5 mm white acrylic #2447	Transmittance = 0.53 Reflectance = 0.10
Clear barrel vault	Length = 1.18 m (46.5”) Width = 0.57 m (22.5”) Height = 0.29 m (11.25”)	Top surface: 3 mm polycarbonate Gables: 13 mm polycarbonate	Transmittance = 0.86 Reflectance = 0.097[(3)]
Tubular skylight	Pipe length = 1.28 m (50.25”) Pipe diameter = 0.254 m (10”) Dome height = 0.11 m (4.25”) Diffuser: flat	Dome: 3 mm acrylic with etched bottom surface. Diffuser: 1 mm acrylic with lenses Pipe: Aluminium	Dome Transmittance = 0.92 Dome reflectance = 0.074 Pipe reflectance = 0.92 Diffuser transmittance = 0.90 Diffuser reflectance = 0.05[(2)]

[(1)] Based on an index of refraction n = 1.49 (Brydson, 1995). It must be noted that the glazing reflectance depends not only on the index of refraction, but also on surface conditions, such as surface roughness, dust accumulation, etc. A value of reflectance = 0.05 was found to yield slightly better results.

[(2)] This is a guessed value since no information was available from the manufacturer.

[(3)] Based on an index of refraction n = 1.6 (Brydson, 1995). However, a value of reflectance = 0.05 was found to yield slightly better results. The polycarbonate glazing was easily susceptible to scratches upon cleaning or wiping.

Figure 6 Clear circular dome as installed on the box roof.

Figure 7 White circular dome as installed on the box roof.

Figure 8 Clear hexagonal pyramid as installed on the box roof.

Figure 9 Clear rectangular bubble as installed on the box roof.

Figure 10 White rectangular bubble as installed on the box roof.

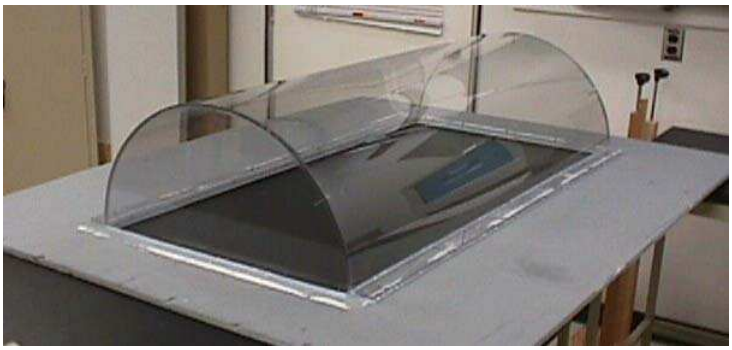

Figure 11 Barrel vault skylight as made in the laboratory.

Figure 12 Tubular skylight as installed on the box roof.

DATA ACQUISITION AND REDUCTION

The LI-COR illuminance sensors and the exhaust fan were connected to an AGILENT data acquisition system. The YANKEE radiometer was connected to a separate data acquisition system belonging to the weather station. The data acquisition system read the sensor signals in voltage and transformed them to the desired units using the sensor calibration curves. Data acquisition was done every minute, and averaged every five minutes. The measurements were taken for a whole day period, covering different sky conditions: overcast, partly cloudy and clear sunny skies. Measurements under rainy or foggy days were discarded.

The measurement results were presented for each sensor reading at each time step in an MS Excel workbook format. The standard time was used. The results were post-processed to get the average values and the graphical plots.

MEASUREMENT PROCEDURE

For the purpose of the measurement quality assurance, the following procedure was undertaken for each skylight setup and each measurement:

On each skylight set up day:

1. Install the skylight.

2. Clean or wipe off the skylight inside and outside surfaces of any dust or water resulting from rain and night time condensation.

3. Clean or wipe the LI-COR exterior illuminance sensor and the YANKEE radiometer if necessary.

4. Place sensors in the correct positions for the skylight transmittance or illuminance measurement.

5. Clean rain water off the floor surface that may have leaked through the roof. The box roof was not completely leak-proof.

6. Plug in the exhaust fan.

7. Synchronize the data acquisition computer clock with the one of the weather station.

8. Start the data acquisition system, and check the data for any questionable values.

On each testing day:

1. Check the exterior skylight surface and sensors, and clean/wipe if necessary in the morning.

2. Record the weather conditions and time whenever there was change in the condition.

SIMULATION METHODOLOGY

To be able to compare the simulation and measurement results, the following inputs were used in simulation:

- Location of the building: the site latitude and longitude as well as the ground/surrounding reflectance.
- Geometry of the measurement box: dimensions and indoor surface reflectances.
- Geometry of the skylight and its dimensions: the width and length of the skylight aperture, and skylight height/raise from its base plane.
- Optical properties (transmittance and reflectance) of the glazing sheet the skylight is made of at normal incidence angle. These inputs are used to calculate the optical properties at oblique incidence angles.
- Measurement day, and the outdoor diffuse and global horizontal illuminances at each time step (five minutes).

Based on these inputs, SkyVision calculates at each time step the floor average illuminance, and the overall skylight optical properties for the sun's beam and diffuse lights. The skylight transmittance for the global light incident on the skylight surface (sun beam, and sky and ground-reflected diffuse lights) is calculated as follows:

$$VT_s = \frac{VT_{beam} \cdot (E_{glob} - E_{dif}) + VT_{dif} \cdot E_{dif}}{E_{glob}} \quad (3)$$

where:

E_{dif} : outdoor horizontal diffuse illuminance (measured);

E_{glob} : outdoor horizontal global illuminance (measured);

VT_{beam} : skylight visible transmittance for the sun beam light for the given sun's altitude angle (simulated);

VT_{dif} : skylight visible transmittance for the sky and ground-reflected diffuse light (simulated); and

VT_s : skylight visible transmittance for the global light (simulated).

RESULT COMPARISON

In the following, the comparison results between the software's predictions and measurements are presented for each skylight shape for both the skylight transmittance and indoor daylight illuminance.

CLEAR DOME SKYLIGHTS

Figure 13 shows a comparison between the measured and simulated skylight transmittance for the clear circular dome skylight on September 17, 2003. Sky conditions were clear and sunny with a few scattered clouds in the early afternoon. The predictions compared very well with the measurements, except at the sunset times where the predictions were slightly higher. This may due to the fact that the measurements had a high uncertainty at very low sun altitude angles (sensor cosine uncertainty is very large at sun altitude angles lower than 10^{o}), and the five sensors may not be enough to represent the transmitted light accurately, especially the inter-reflected component. Transmission by inter-reflection occurs at the lower part of the skylight surface and is more significant at low sun altitude angles. Sensors placed close to the skylight surface would capture the inter-reflected light.

Figure 14 shows the uniformity of the illuminance under the skylight as measured by the five illuminance sensors. Although, the sensors readings seem close to each other, particularly at off-noon times, the use of one sensor to measure the skylight visible transmittance as in the ASTM standard E972-96 (or E1084-86/96) would introduce an uncertainty of about 5% in the calculations, compare the middle sensor reading with average one, for example.

Figures 15 to 17 show a comparison between the measured and simulated floor average illuminance for the clear circular dome skylight under partly cloudy and overcast sky conditions. The predictions compared very well with the measurements, particularly for the overcast sky conditions. The difference between the simulated and measured values was due to two main error sources. First, the outdoor diffuse and global illuminance measurements, which were measured by the YANKEE system and used in the simulation, were not completely synchronized with the measurements of the indoor illuminances (time delay or advance was in the order of 1 to 3 minutes). This time delay/advance had a significant impact in the simulation, especially for highly changing sky conditions such as the partly cloudy conditions in Figure

15. Second, the use of 16 illuminance sensors was perhaps not enough to fully represent the average illuminance.

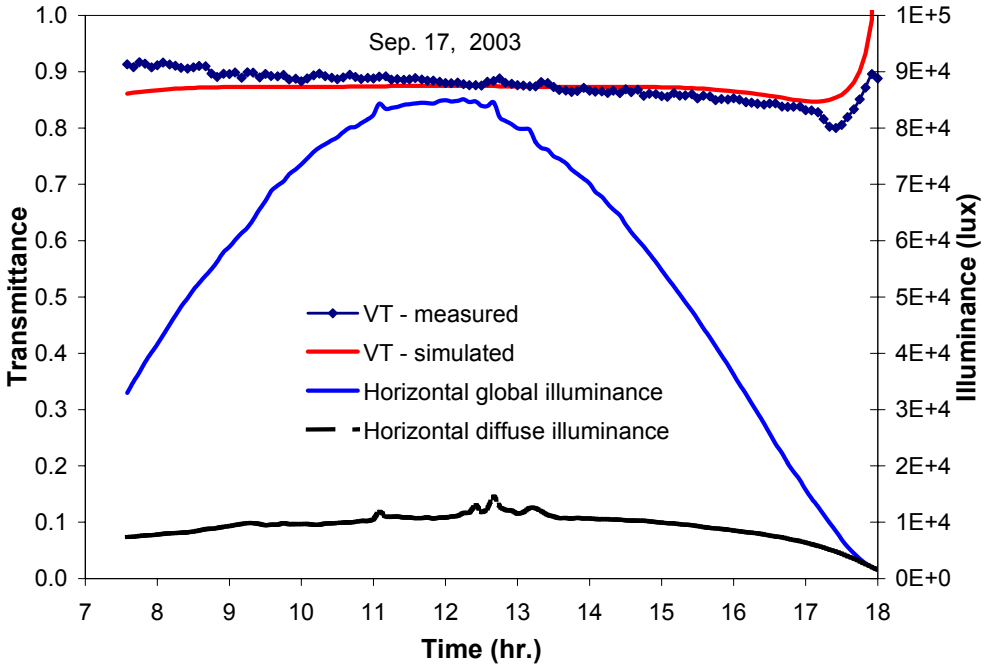

Figure 13 Profiles of the measured and simulated skylight visible transmittance (VT) as a function of daytime - clear circular dome.

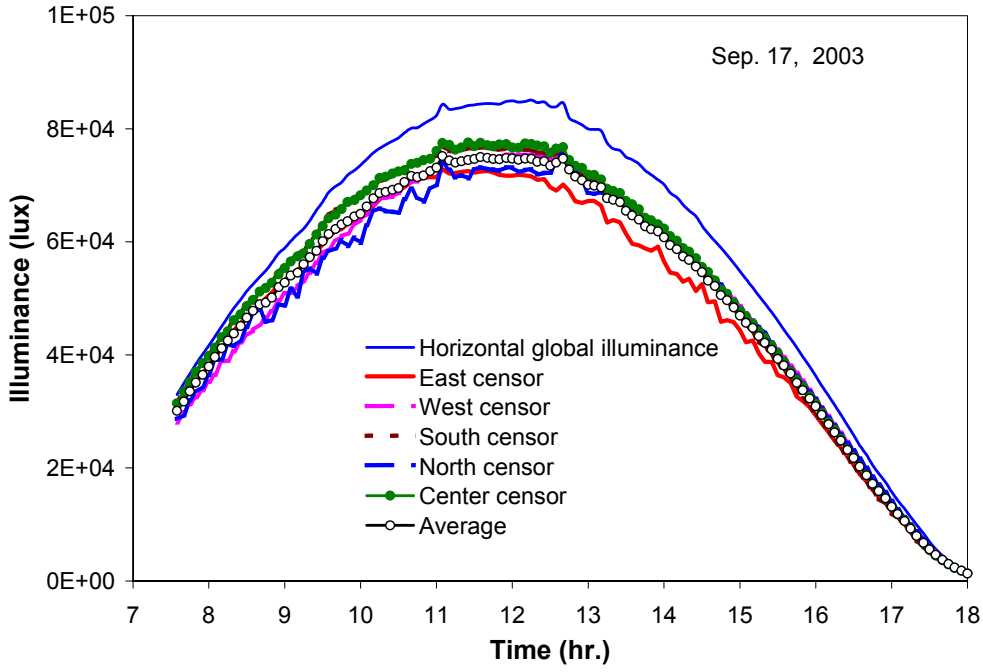

Figure 14 Illuminance uniformity under the skylight - clear circular dome.

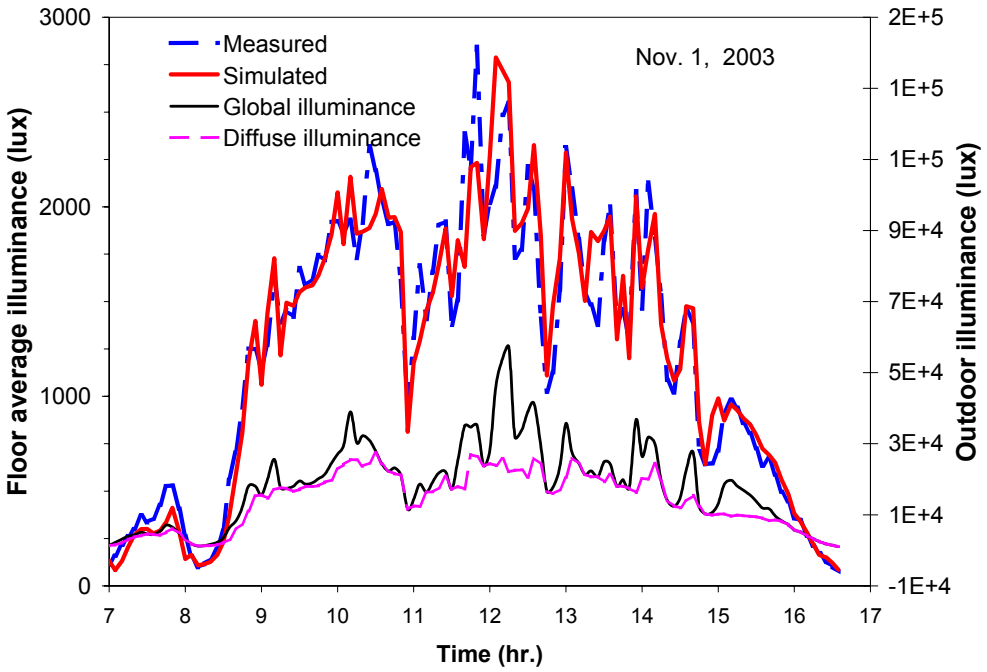

Figure 15 Profile of the floor average illuminance as a function of daytime under a partly cloudy sky - clear circular dome.

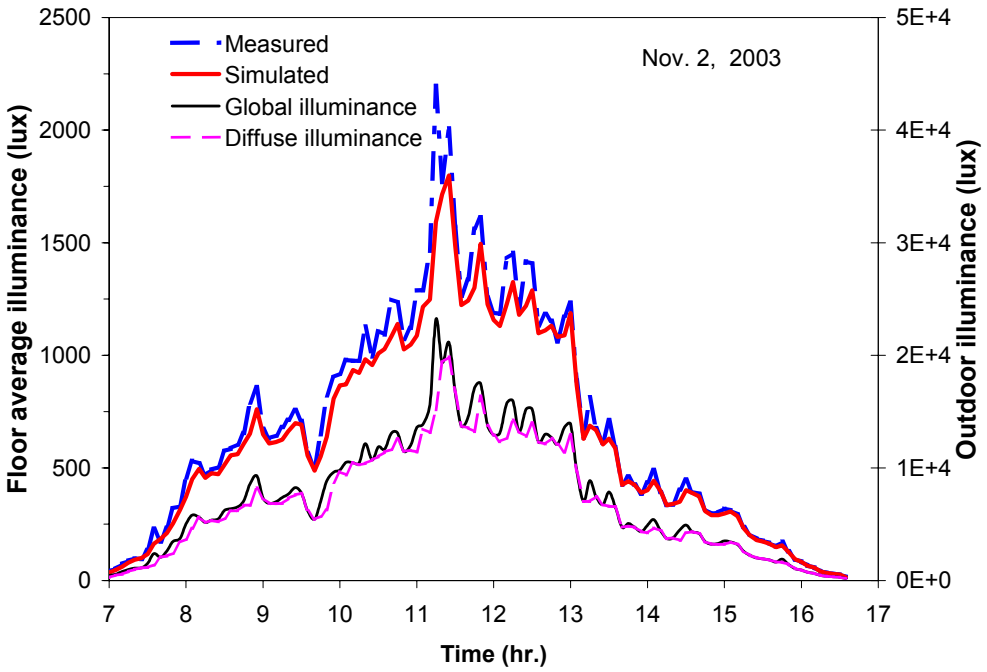

Figure 16 Profile of the floor average illuminance as a function of daytime under an overcast sky - clear circular dome.

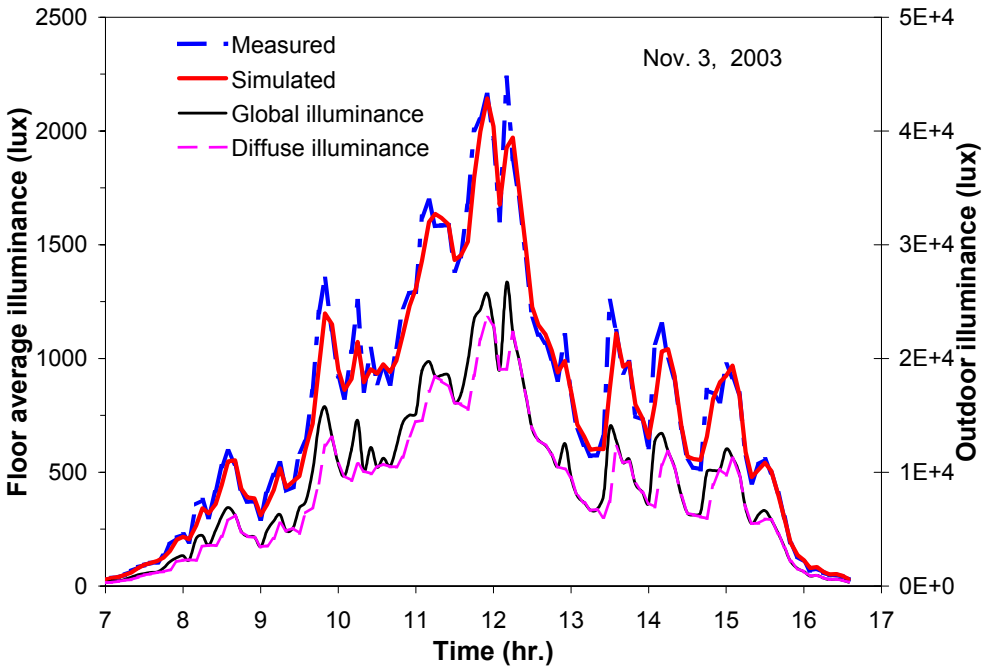

Figure 17 Profile of the floor average illuminance as a function of daytime under an overcast sky - clear circular dome.

DIFFUSE DOME SKYLIGHTS

Figure 18 shows a comparison between the measured and simulated skylight transmittance for the diffuse (white) circular dome skylight on September 24, 2003. Sky conditions were clear in the morning, overcast around noontime, and partly cloudy in the afternoon. The predictions compared very well with the measurements, except at the sunset times where the predictions were about 10% higher than the measurements. This difference was mainly due, as described above, to the time lag between the weather station readings and the indoor illuminance measurements, the high measurement uncertainty at very low sun's altitude angles, and the number of sensors.

Figure 19 shows the uniformity of the illuminance under the skylight as measured by the five illuminance sensors. The sensor positions under this diffuse skylight had a significant impact on the sensor readings, particularly under clear or partly cloudy sky conditions. Sensors placed under the exposed skylight surface (surface directly hit by the sun's rays) measured higher values than the ones placed under the non-exposed surface area. The sensor readings were sometimes higher than the outdoor ones due to the ground reflected light. For example, under the clear sky conditions in the morning, the east and south sensors measured higher values than the west and north sensors. The east sensor measured higher values than the outdoor around the sunrise time. The situation was inversed under the partly cloudy sky conditions in the afternoon. The middle sensor measured about 12% higher values than the average of

the five sensors. This suggests that for diffuse skylights, an adequate number of sensors should be used to measure the average illuminance under the skylight.

Figure 20 shows a comparison between the measured and simulated floor average illuminance for the white circular dome skylight. The sky conditions were partly cloudy all day. The predictions were in excellent agreement with the measurements.

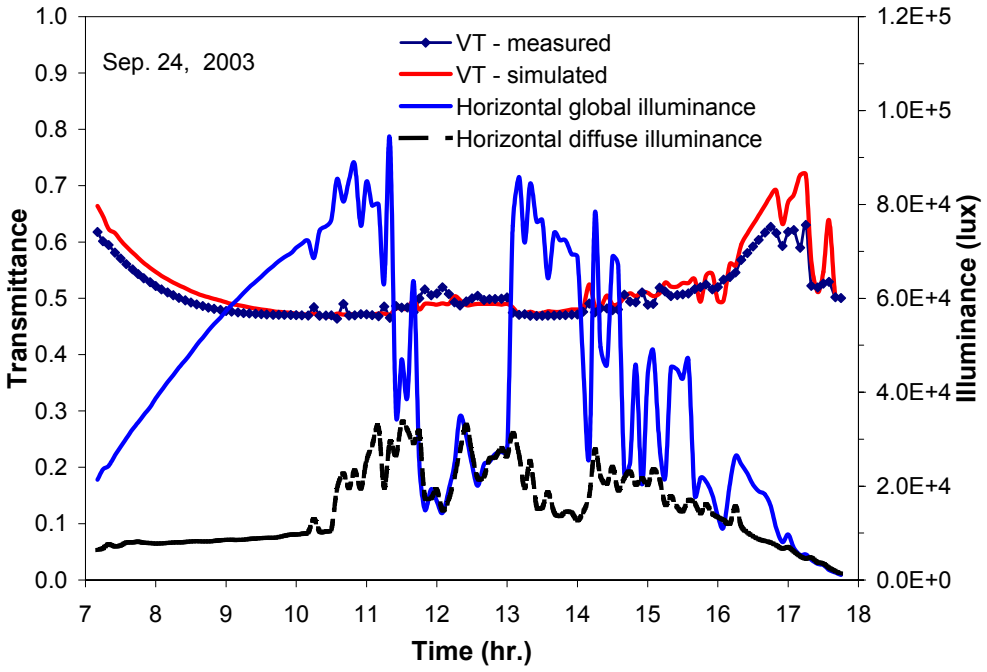

Figure 18 Profile of the skylight visible transmittance (VT) as a function of daytime - diffuse circular dome.

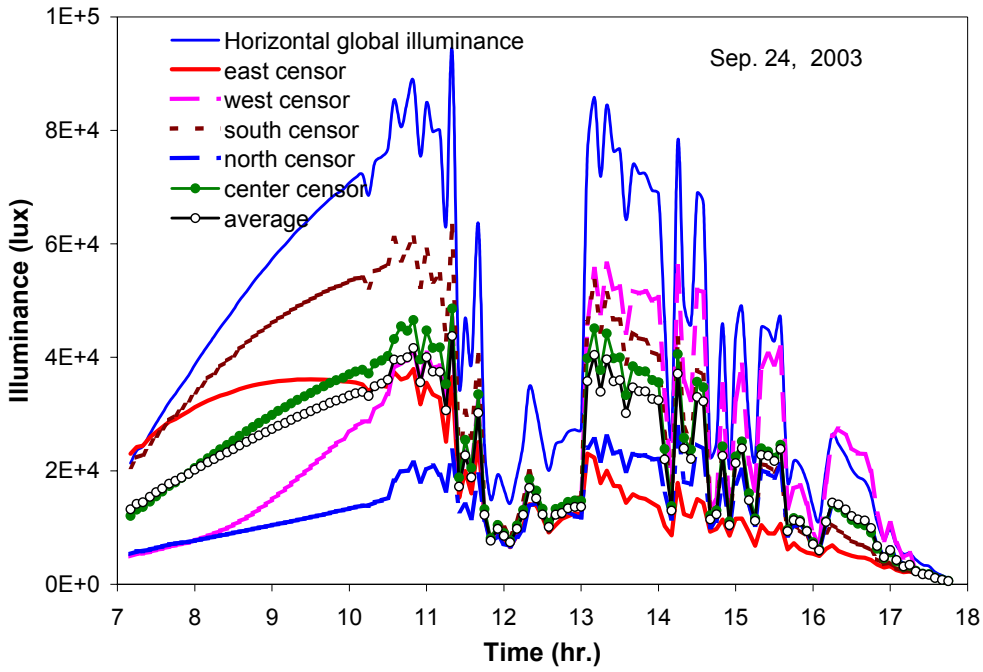

Figure 19 Illuminance uniformity under the skylight - diffuse circular dome.

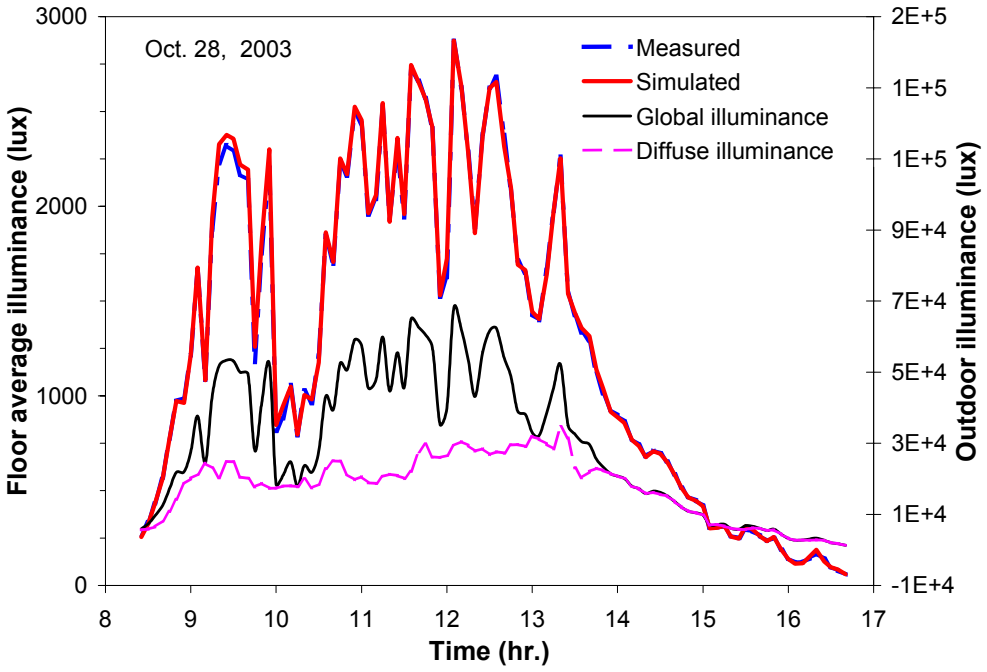

Figure 20 Profile of the floor average illuminance as a function of daytime under a partly cloudy sky - diffuse circular dome.

CLEAR PYRAMIDAL SKYLIGHT

Figures 21 to 23 show a comparison between the measured and simulated skylight transmittance for the clear hexagonal pyramid under partly cloudy, mostly overcast and clear sky conditions, respectively. Contrary to the previous results for the clear dome skylight, the measured transmittance of the clear hexagonal pyramid exhibited an unusual behaviour, particularly under sunny sky conditions. The measured transmittance oscillated between low and high values within a period of about 20 to 40 min, depending on the sun position in the sky. When the sensor readings were closely examined, it was found that some of the sensors measured much higher or lower illuminances than the others, sometimes higher than the outdoor illuminance. When the sun's rays hit the surface vertices of the pyramid, alternating darker and brighter segments of about ½" wide were cast on some of the sensors. The darker segments corresponded to the thickest portion of the surface vertex, and brighter segments corresponded to the thinnest portion. This observation suggests a lens effect along the vertices of the pyramid surfaces. Consequently, the software's predictions were about 30% lower than the measurements, particularly under clear sky conditions. Under overcast skies, predictions were about 6% lower than the measurements.

The aforementioned lens effect is clearly shown in Figures 24 to 26. The sensor readings were extremely erratic, continuously oscillating from a lowest to a highest value within a short period of time. For example, under sunny sky conditions (Figures 24 and 26) the west sensor measured about 60% more than the average of the five sensors, and about 50% more than the outdoor illuminance. On the credit side, this lens effect is desirable since it boosts the skylight transmittance. On the debit side, however, skylights with such effects may cause an excessive glare problem, and make affect the correct operation of a daylight-linked lighting control system. To overcome this localized lens effect (which is due to the curvature and non-uniform thickness of the skylight glazing panes), skylights should be multi-pane with at least one diffusing glazing, or they should be employed with a well diffuser.

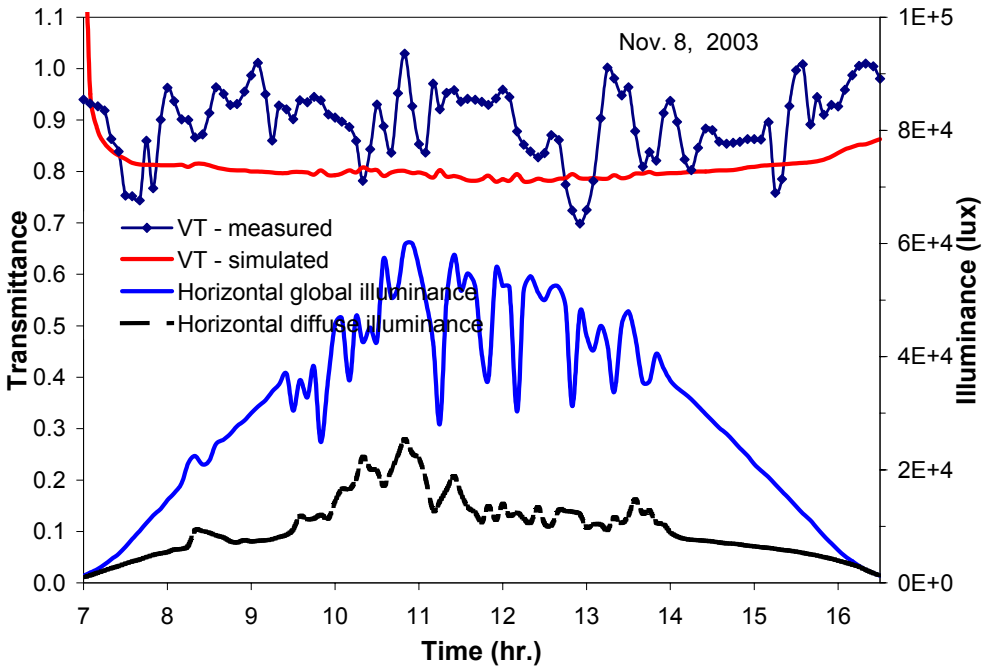

Figure 21 Profile of the skylight visible transmittance (VT) as a function of daytime under a partly cloudy sky - clear pyramid.

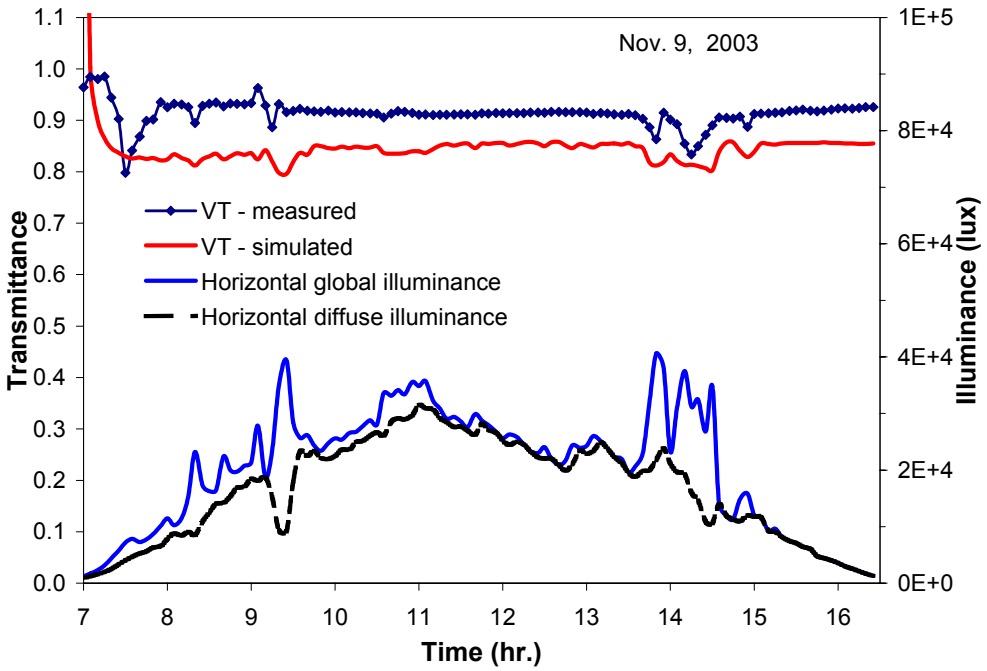

Figure 22 Profile of the skylight visible transmittance (VT) as a function of daytime under an overcast sky - clear pyramid.

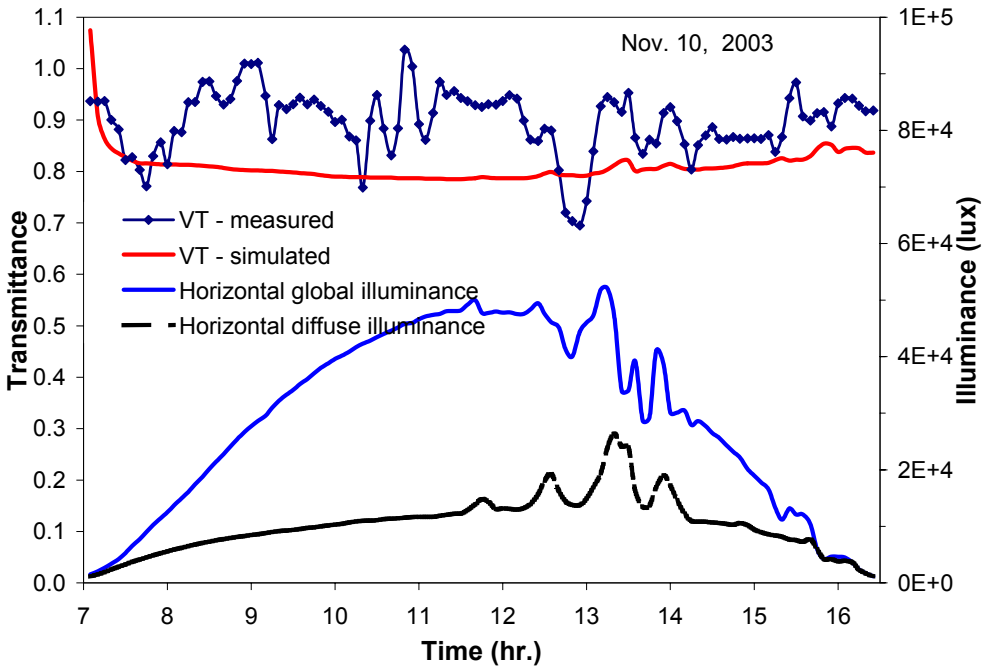

Figure 23 Profile of the skylight visible transmittance (VT) as a function of daytime under a sunny sky - clear pyramid.

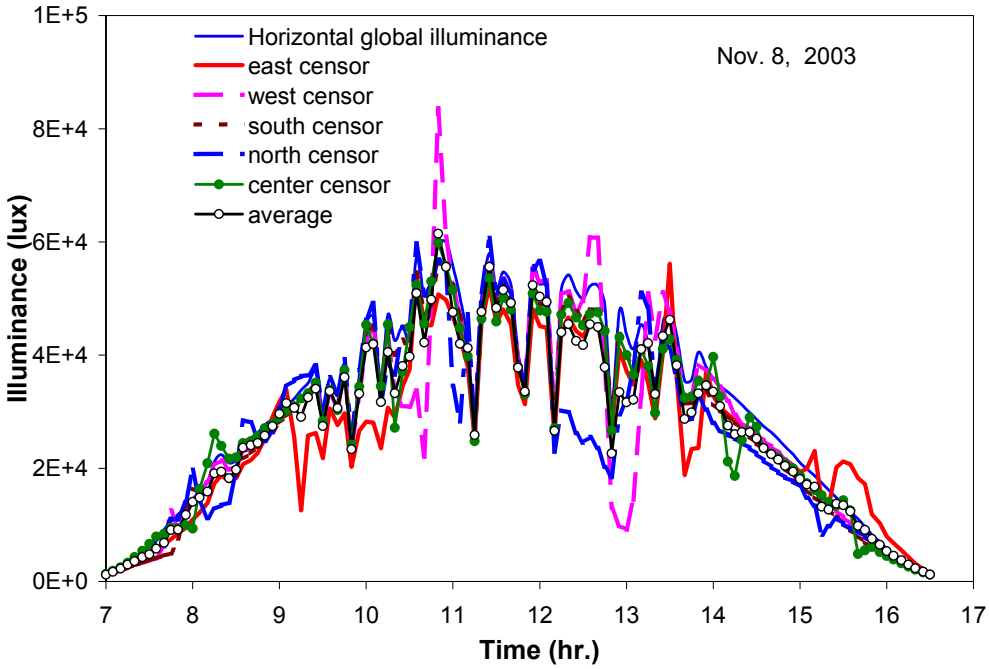

Figure 24 Illuminance uniformity under the skylight of a partly cloudy sky - clear pyramid.

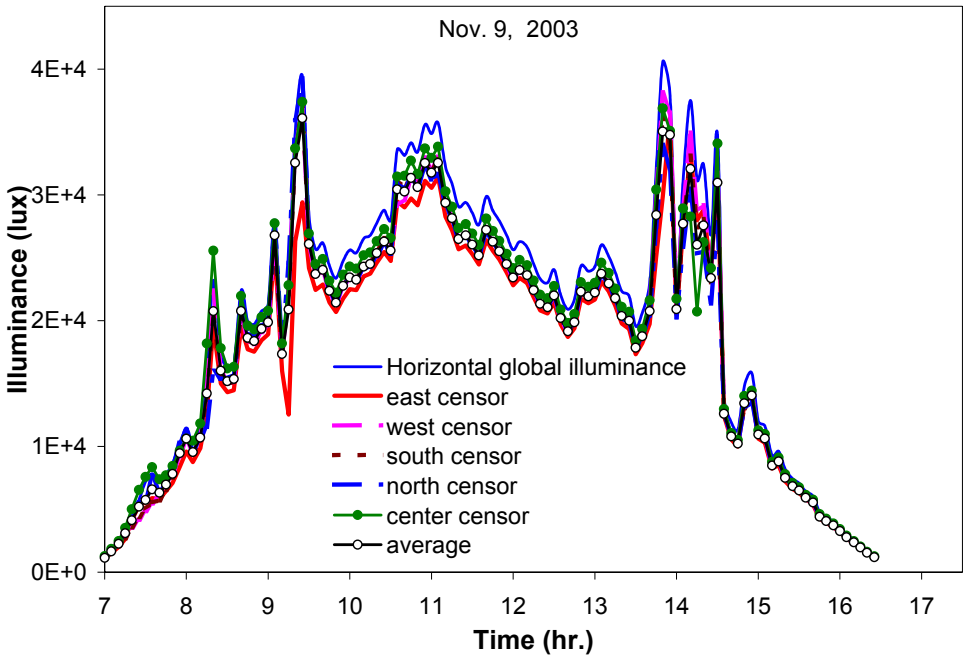

Figure 25 Illuminance uniformity under the skylight of an overcast sky - clear pyramid.

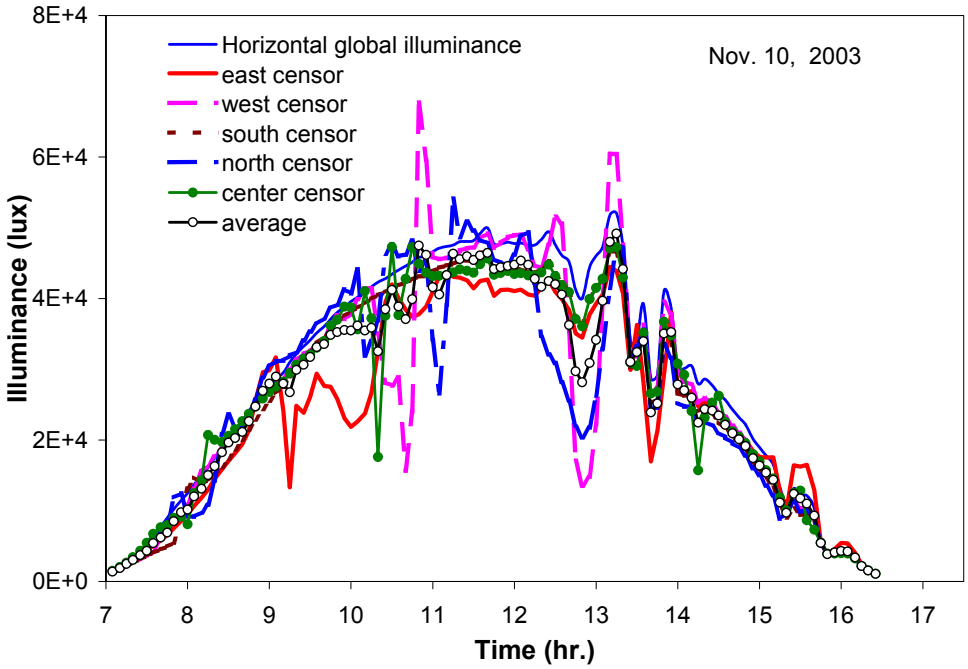

Figure 26 Illuminance uniformity under the skylight of a sunny sky - clear pyramid.

CLEAR BUBBLE SKYLIGHT

Figures 27 and 28 show a comparison between the measured and simulated skylight transmittance for the clear rectangular bubble skylight on October 6 and 7, 2003, respectively. On October 6, the sky conditions were mostly overcast in the morning, partly cloudy in the afternoon (about 60% cloud cover), and sunny at sunset. On October 7, the sky conditions were sunny in the morning, and partly cloudy in the rest of the day. The predictions compared very well with the measurements, with a maximum difference less than 5%. This uncertainty was attributed primarily to the fact that the five sensors might not be enough to represent the transmitted energy accurately, especially the inter-reflected component. Transmission by inter-reflection occurs at the lower part of the skylight surface and is more significant at low sun's altitude angles. Sensors placed close to skylight surface would capture the inter-reflected light.

Figures 29 and 30 show the uniformity of the illuminance under the skylight as measured by the five illuminance sensors. Under the partly cloudy sky conditions, the sensors reading were almost identical, particularly at off sunset/sunrise times. When the sky conditions were clear in the morning (e.g., Figure 30), the sensor readings were more different. The north sensor measured about 12% higher illuminance than the outdoor at around 9:00 AM, indicating probably a strong inter-reflection from the skylight inside surface. The south sensor, which did not receive inter-reflection, measured about 26% lower value than the average.

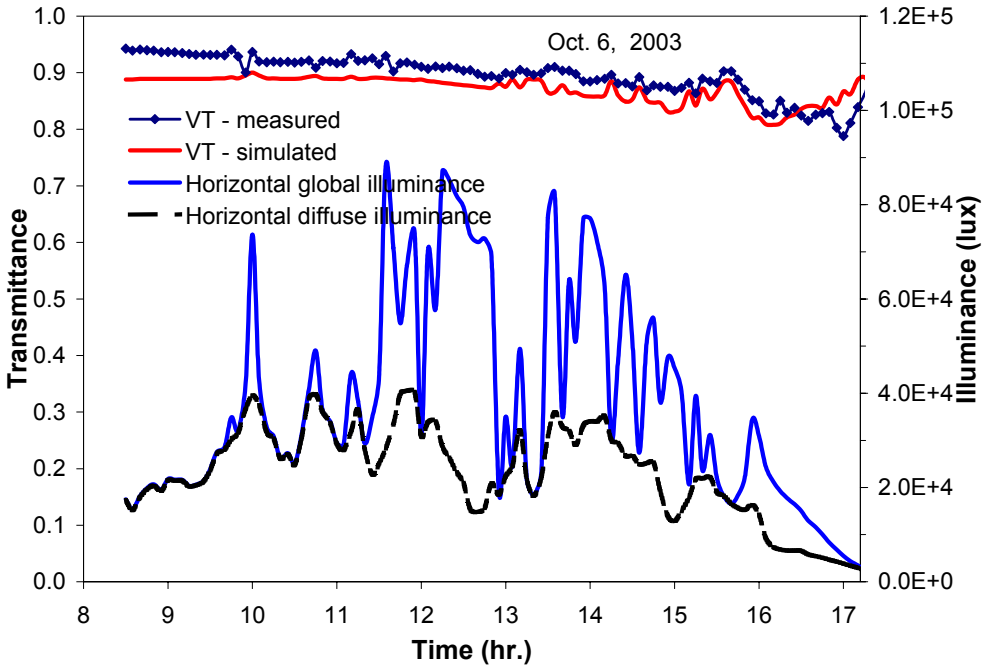

Figure 27 Profile of the skylight visible transmittance (VT) as a function of daytime under a partly cloudy sky - clear rectangular bubble.

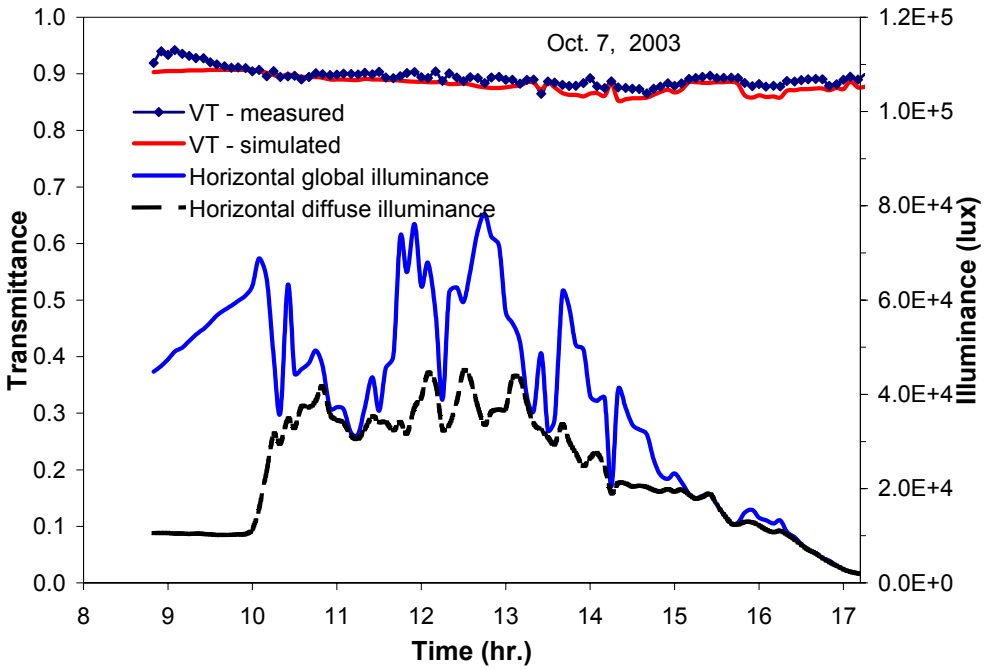

Figure 28 Profile of the skylight visible transmittance (VT) as a function of daytime under a partly cloudy sky - clear rectangular bubble.

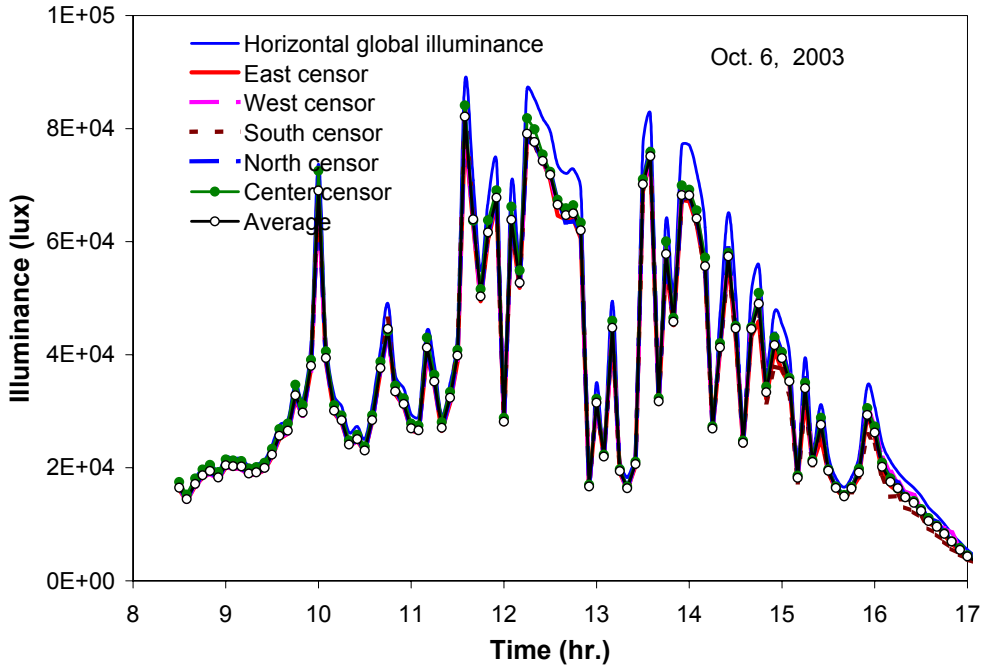

Figure 29 Illuminance uniformity under the skylight of a partly cloudy sky - clear rectangular bubble.

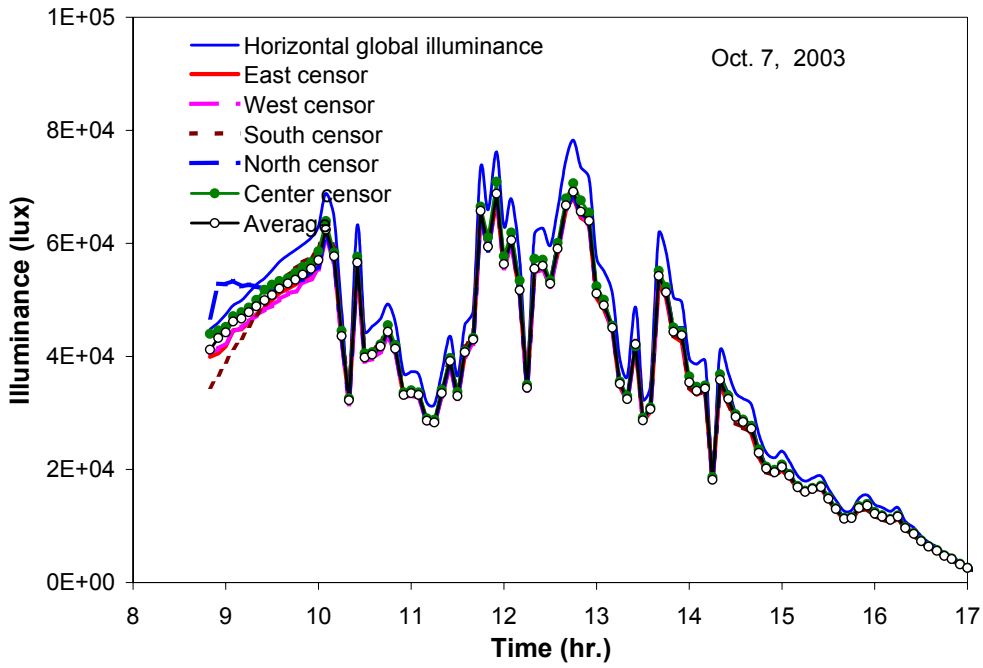

Figure 30 Illuminance uniformity under the skylight of a partly cloudy sky - clear rectangular bubble.

DIFFUSE BUBBLE SKYLIGHT

Figure 31 shows a comparison between the measured and simulated skylight transmittance for the diffuse (white) rectangular bubble skylight on October 9, 2003. Sky conditions were hazy in the morning, overcast around noontime (sun not visible), and sunny with a little haze in the late afternoon. Overall, the predictions compared well with the measurements, particularly on clear sky conditions (e.g., at late afternoon). The maximum difference between the measurements and predictions was less than 11%. This difference was perhaps due to the number of sensors not being adequate to represent the transmitted energy.

Figure 32 shows the uniformity of the illuminance under the skylight as measured by the five illuminance sensors. The sensor positions had a significant impact on the sensor readings, particularly under clear or hazy sky conditions. Sensors placed under the exposed skylight surface (surface directly hit by the sun's rays) measured higher values than the ones placed under the non-exposed surface area. For example, under the clear sky conditions in the late afternoon, the west and south sensors measured higher values than the east and north sensors. The situation was inversed under the hazy sky conditions in the morning. The middle sensor, surprisingly, measured approximately the same values as the average of the five sensors.

Figures 33 to 34 show a comparison between the measured and simulated floor average illuminance for the white rectangular bubble skylight under partly cloudy conditions. The predictions compared very well with the measurements, with a maximum uncertainty less than 9%. This difference was likely due to the use of only 16 illuminance sensors to represent the average illuminance.

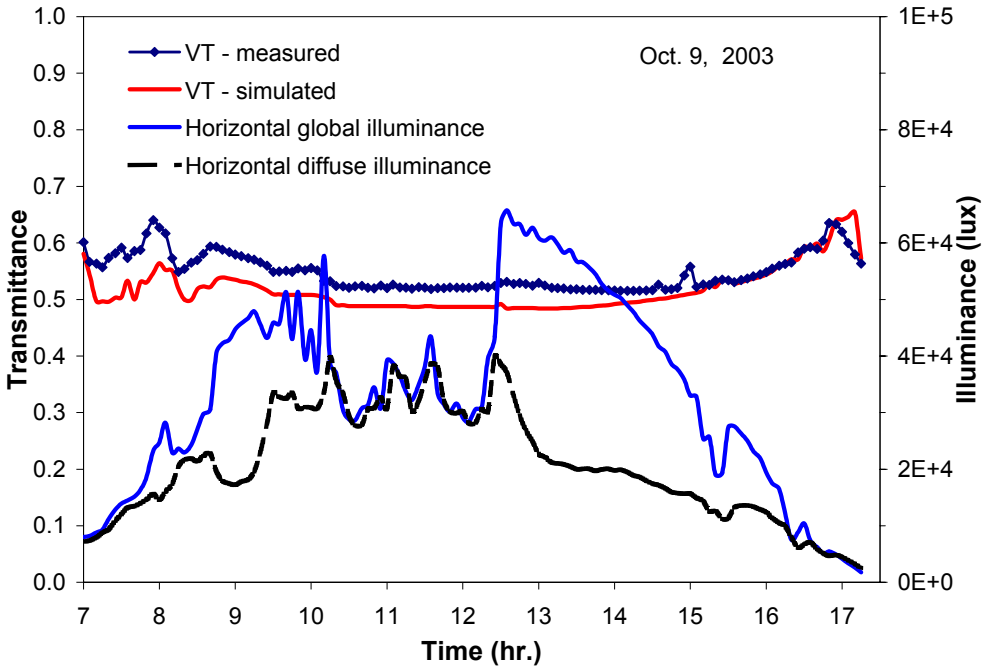

Figure 31 Profile of the skylight visible transmittance (VT) as a function of daytime – diffuse rectangular bubble.

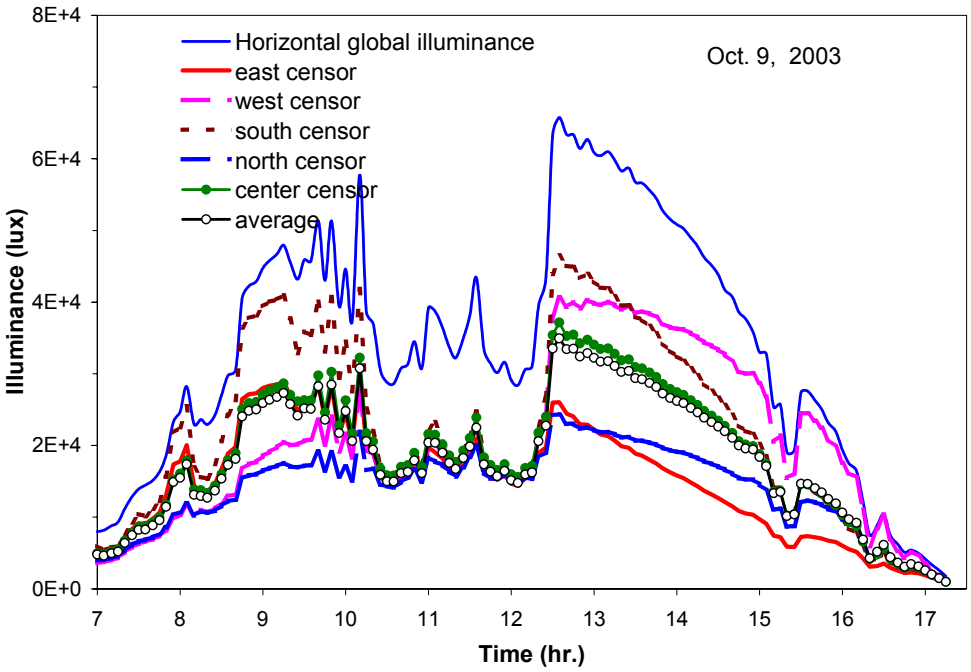

Figure 32 Illuminance uniformity under the skylight of a partly cloudy sky - diffuse rectangular bubble.

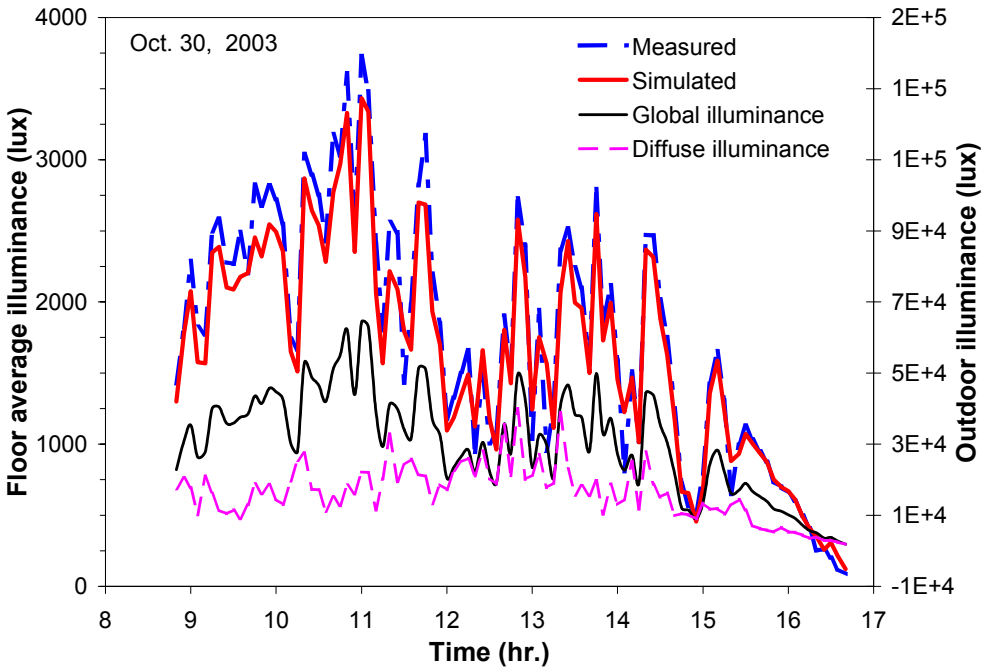

Figure 33 Profile of the floor average illuminance as a function of daytime under a partly cloudy sky - diffuse rectangular bubble.

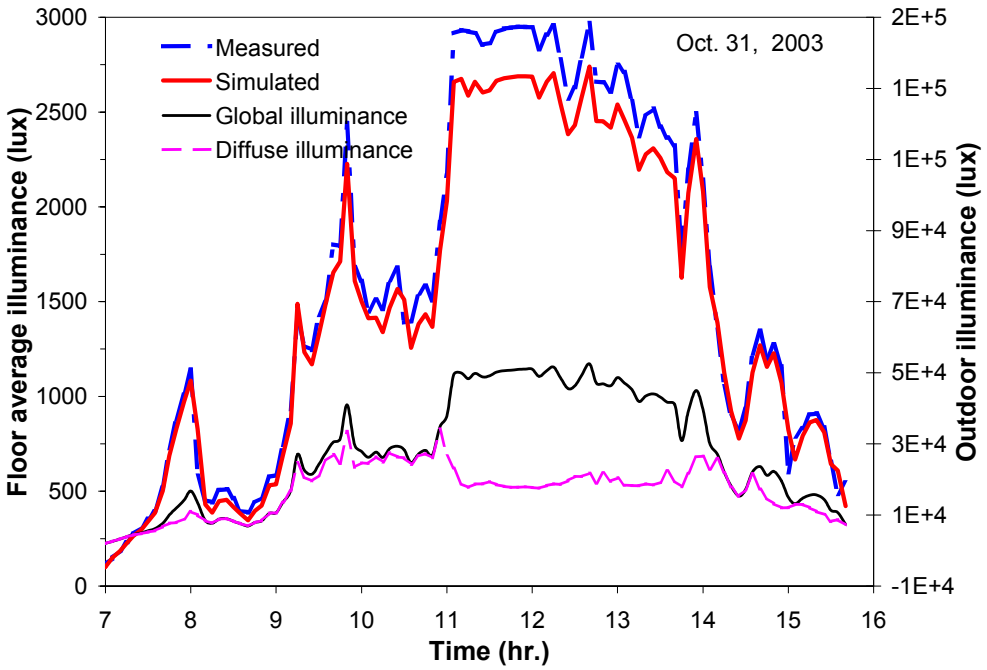

Figure 34 Profile of the floor average illuminance as a function of daytime under an overcast sky - diffuse rectangular bubble.

CLEAR BARREL VAULT SKYLIGHT

Figure 35 shows a comparison between the measured and simulated skylight transmittance for the clear barrel vault skylight on October 24, 2003. Sky conditions were partly cloudy in the morning and mostly sunny in the afternoon. The predictions were in excellent agreement with the measurements, except at sunset where the measurements had high uncertainty due to sensor cosine response sensitivity.

Figure 36 shows the uniformity of the illuminance under the skylight as measured by the five sensors. The sensor readings were very similar, except when the sun's rays hit the vertices between the top cylindrical surface and the end walls. The middle sensor readings deviated about 2% from the average of the five sensors.

Figures 37 to 38 show a comparison between the measured and simulated floor average illuminance for the clear barrel vault skylight under partly cloudy and mostly overcast sky conditions, respectively. The predictions compared very well with the measurements, with a maximum uncertainty less than 11%. The difference was mainly due to fact that the outdoor illuminance measurements, which were measured by the YANKEE system and used in the simulation, were not completely synchronized with the measurements of the indoor illuminances. The time difference between both measurements had a significant impact in the simulation, especially for highly changing sky conditions such as the partly cloudy conditions of Figure 37.

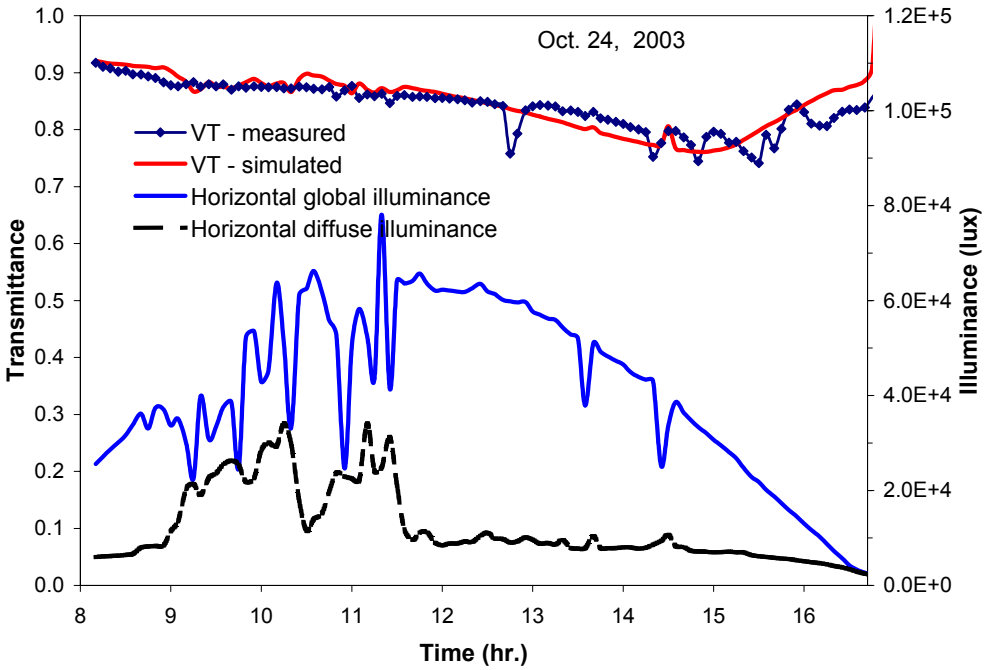

Figure 35 Profile of the skylight visible transmittance (VT) as a function of daytime – clear barrel vault.

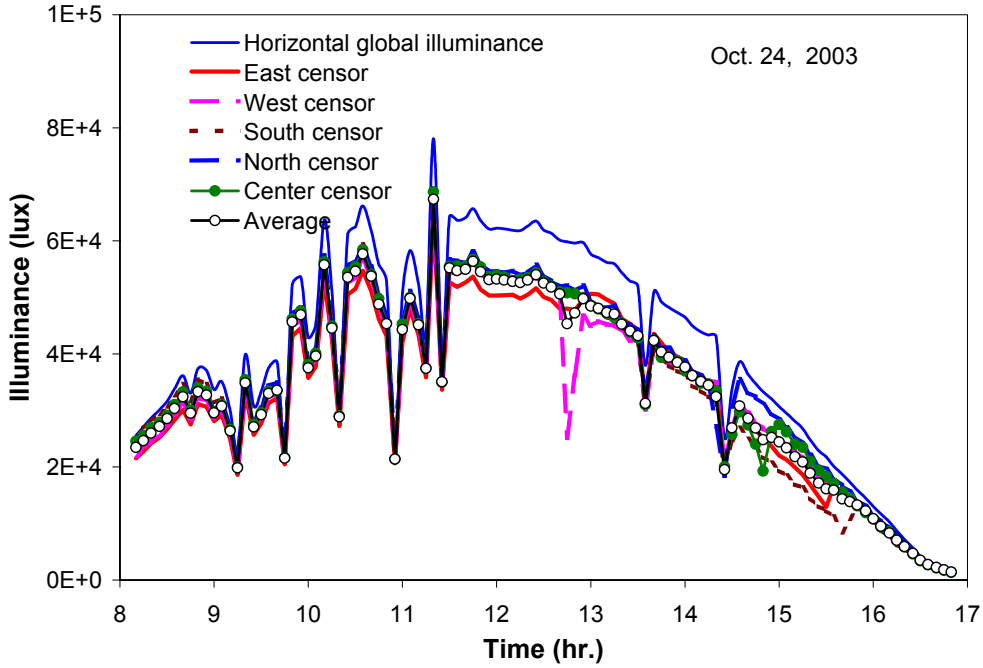

Figure 36 Illuminance uniformity under the skylight of a partly cloudy sky - clear barrel vault.

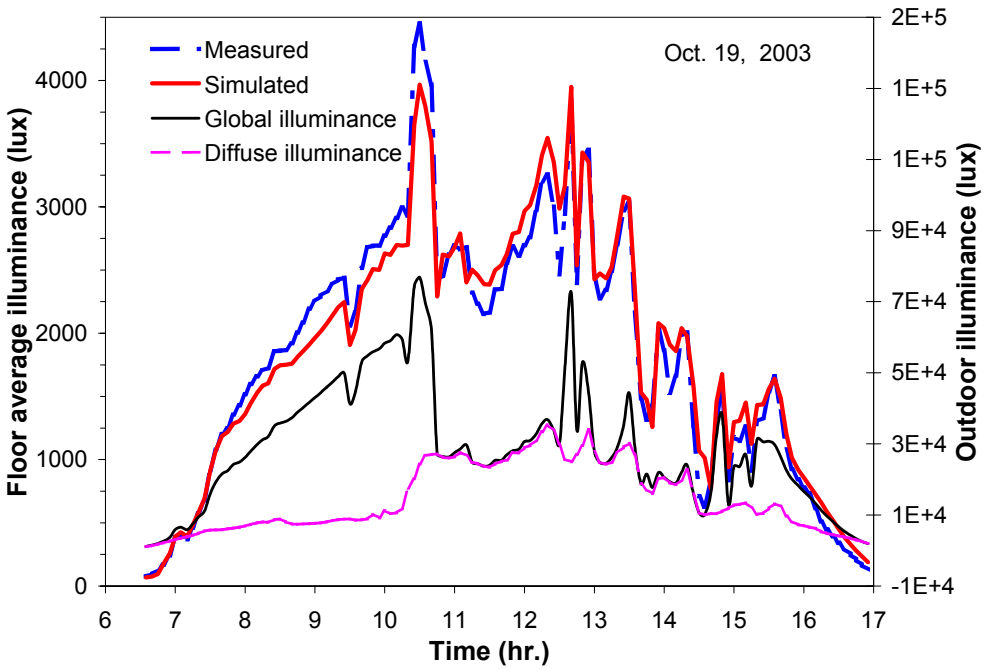

Figure 37 Profile of the floor average illuminance as a function of daytime under a partly cloudy sky - clear barrel vault.

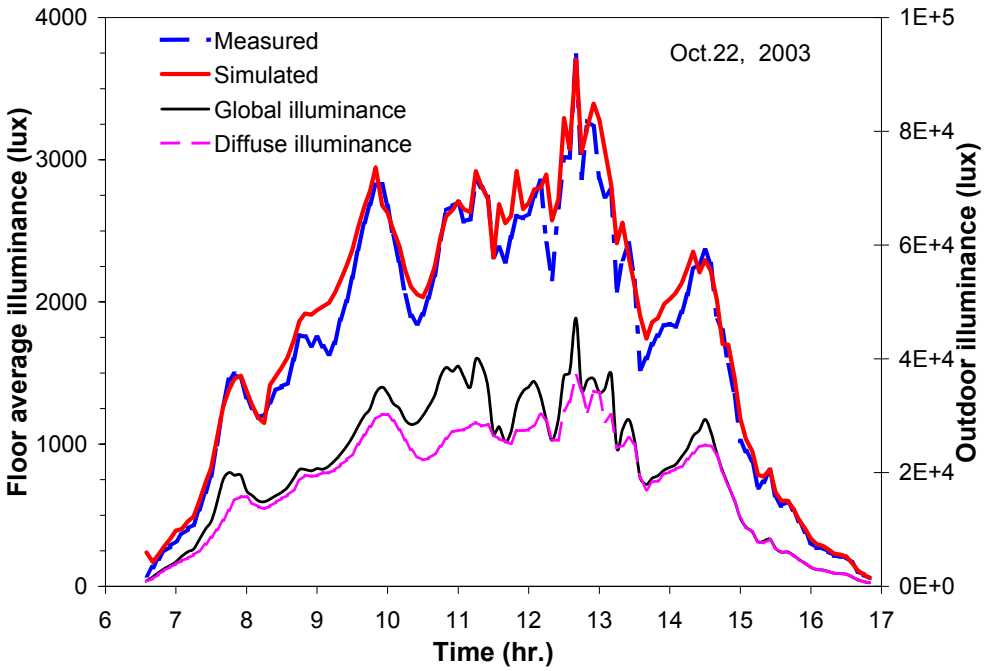

Figure 38 Profile of the floor average illuminance as a function of daytime under a mostly overcast sky - clear barrel vault.

TUBULAR SKYLIGHT

The transmittance measurement of the tubular skylight used only one illuminance sensor placed 2" (5 cm) below the middle of the diffuser. The decision to use only sensor stemmed from the fact if the diffuser behaves as (or mimics) a perfect diffuser, then one sensor with an acceptable view angle would be sufficient to capture the light flux exiting the diffuser (ASTM Standard E1084). However, it turned out that the skylight diffuser, which incorporated some Frenel lenses for diffusion, did not equally spread light in all directions. Depending on the sun altitude angle, the diffuser may have diffused more light off the centre line, causing the illuminance sensor to measure less light output. The use of one sensor to measure the transmittance of lightpipes is therefore not an accurate method, particularly under clear sky conditions. Following the client request, the measurement data was not presented in this report. Data from published sources were instead used for the comparison.

Several studies have been conducted to measure/predict the performance of tubular skylights. However, the author could not find any relevant published data for the transmittance of the whole skylight product (collector, pipe and diffuse) in a suitable form for comparison. Previous studies focused mainly on the optical efficiency of the pipe only, or the dome plus pipe. Zastrow and Wittmer (1986) developed a simple relation to predict the pipe transmittance, given in the following equation:

$$VT_{pipe} = \rho^{4/\pi \cdot L/D \cdot \tan\theta} \tag{4}$$

where:

D : pipe inner diameter;

L : pipe length;

θ : incidence angle with respect to the pipe's axis; and

ρ : pipe reflectance.

Swift and Smith (1995) developed a theoretical complex model to compute the pipe transmittance. They also conducted laboratory measurements, which compared generally well with the model predictions. Chao (1996) developed a simple formula for the pipe transmittance, given in the following form:

$$VT_{pipe} = \frac{e^{L/D \cdot \tan\theta \cdot Ln(\rho)}}{\sqrt{1 - L/D \cdot \tan\theta \cdot Ln(\rho)}} \tag{5}$$

Figure 39 shows a comparison between the previous models and SkyVision in predicting the profile of the pipe transmittance. The pipe inner surface was assumed specular with a constant reflectance equal to 0.95. The pipe aspect ratio L/D was varied from one to eight. All the models compared very well with each others, except the model by Chao (1996), which under-predicted the pipe transmittance by up to 10%. Despite its simplicity, the Zastrow and Wittwer (1986) model gave very good results for the covered pipe aspect ratios.

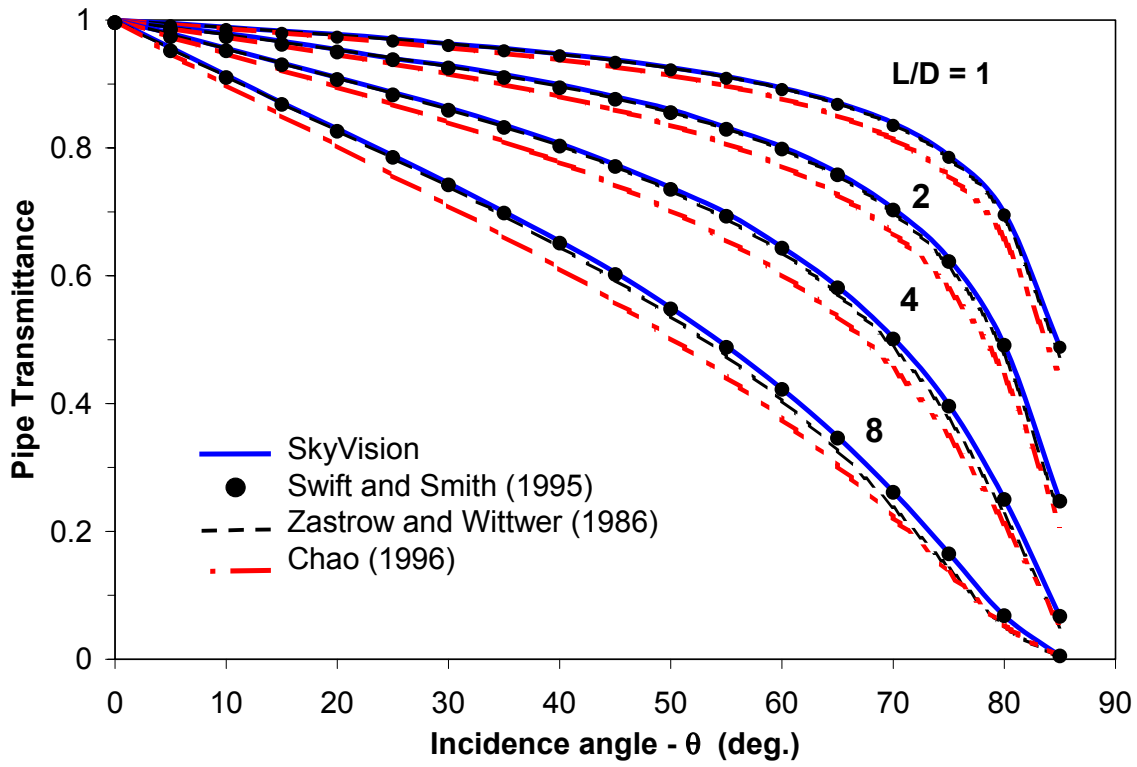

Figure 39 Profile of the pipe transmittance as a function of the incidence angle

COMPARISON WITH THE PIER RESULTS

The California Energy Commission conducted, through the PIER (Public Interest Energy Research) program, extensive measurements on the visible transmittance, solar heat gain coefficient, and U-value of a number of skylight and well combinations. Twenty four tests were carried out to measure the effective visible transmittance of skylight and well combinations. Three skylight types were tested: a flat model with clear glazing; a square bubble (dome) model with multi-pane clear or diffuse glazing; and a square pyramid model with multi-pane clear glazing. Two types of light wells with varying heights were considered: a diffuse well and a specular (mirror-like) well.

The measurements included the visible transmittance of the flat sheet the skylight is made of, and the effective transmittance of the skylight plus well combinations. Two methods were used to measure the effective transmittance of skylights: the calorimeter box method and the photometry method. In this report only the results from the calorimeter box method were used for the comparison. More details may be found in McHugh et al. (2004).

To measure the effective transmittance of skylights, sixteen illuminance sensors were uniformly deployed on the well floor surface. Two additional outdoor sensors were used to measure the global illuminance on horizontal and 20^{o} inclined surfaces. The diffuse outdoor illuminance was not, however, measured. The measurements were conducted in the city of Tempe, AZ on the Arizona State University Campus (latitude N 33.4^{o}, longitude W 112.9^{o}). The effective transmittance was calculated as the ratio of the light flux reaching the well floor surface to the one incident on the rough opening of the skylight.

The comparison results in this report included only skylights that were fully transparent or translucent (diffuse) because the current version of SkyVision handles only these types of glazing. Table 2 summarizes the physical characteristics of the tested skylights used for the comparison, and Table 3 summarizes the physical characteristics of the curb and well spaces as used in the simulation.

SIMULATION ASSUMPTIONS

The following assumptions were used in the simulation:

- The sky conditions for all measurements were clear. The CIE standard clear sky condition was used to compute the outdoor global and diffuse illuminances for the measurement location. Local sky conditions may, however, deviate from the standard ones.

- Simulations results for the specular well and skylight combinations were obtained using the lightpipe model in SkyVision. Since SkyVision does not provide an option to simulate a diffuse curb and specular well combination, the diffuse curb effect was accounted for by multiplying the skylight glazing transmittance by the curb efficiency, which was equal to 0.89 (calculated). This is actually an

approximation and it should not be considered as an accurate method in dealing with this type of curb/well combination.

- Simulations for the double clear-over-diffuse bubble dome were obtained assuming a constant transmittance of the flat sheet equal to the measured one at normal incidence angle, since the current version of SkyVision does not include skylights with a mixture of clear and diffuse glazing. This assumption should be valid up to an incidence angle on a horizontal surface of 40^{o}. Significant error is expected at higher incidence angles (or low sun elevations).

- The ground/surrounding reflectance was fixed to 0.2.

Based on the aforementioned inputs, SkyVision calculated the effective transmittance of the skylight as the ratio of the average illuminance of the well floor surface to the outdoor global horizontal illuminance. It should be noted that this definition differs from the one in the PIER report by the area ratio of the well opening to skylight rough opening, which was about 0.98.

In the following, the software's predictions are compared with the measurements of each skylight and well combination.

Table 2 Physical characteristics of the tested skylights in the PIER program. The optical properties of the glazing sheet the skylight is made of were measured at normal incidence angle, unless otherwise stated.

Skylight Shape	Interior Dimensions	Material	Optical Properties (visible spectrum)
Single diffuse bubble	Length = 1.194 m (47”) Width = 1.194 m (47”) Height = 0.3 m (12”)	3 mm white acrylic	Transmittance = 0.626 Reflectance = 0.10[2]
Single clear pyramid	Length = 1.194 m (47”) Width = 1.194 m (47”) Height = 0.096 m (3.77”)	3 mm bronze acrylic	Transmittance = 0.282 Reflectance = 0.04[1]
Double diffuse bubble	Length = 1.194 m (47”) Width = 1.194 m (47”) Height = 0.196 m (7.7”)	3 mm clear acrylic (outside) 3 mm white acrylic (inside)	Total Transmittance = 0.594 Total Reflectance = 0.1[2]
Double clear low-e flat skylight [3]	Length = 1.194 m (47”) Width = 1.194 m (47”)	6 mm clear float glass (pane ID = 103) 6 mm low-e glass (pane ID = 3104) (inside)	Total Transmittance = 0.467 Total Reflectance = 0.10[3]

[1] Based on an index of refraction n = 1.49.

[2] This is a guessed value since no information was provided in the report.

[3] Since there was no information in the report on the material making up the double low-e glazing, the optical properties were taken from the glass database of the WINDOW5 program that yielded approximately the same visible transmittance as the measured one at normal incidence angle.

Table 3 Physical characteristics of the curb and well spaces as used in the simulation.

Space	Interior Dimensions	Reflectance
Curb	Height = 0.09 m (3.5”)	Wall: 0.35 (typical lumber wood)
Diffuse Well	Height = variable	Wall: 0.81 Floor (black paint): 0.10
Specular Well	Height = variable	Wall: 0.95 Floor (black paint): 0.10

SINGLE DIFFUSE BUBBLE SKYLIGHT

Figure 40 shows a comparison between the measured and simulated skylight effective transmittance for the combination of a single-glazed diffuse bubble dome and diffuse well. The predictions and measurements followed the same trend. The effective transmittance decreases with increasing sun elevation angles, and with increasing well height. The measurement data for the 6-foot well seemed erroneous since they were higher than the ones for the 3-foot well at low sun's altitude angles. Overall, the predictions compared well with the measurements for the 1- and 3-foot wells. The maximum error was less than 9%. This error may be attributed to the reflectance value of the curb and well surfaces, which were not measured.

Figure 41 shows a comparison between the measured and simulated skylight effective transmittance for the combination of a single-glazed diffuse bubble dome and specular well. The predictions and measurements followed the same trend. The effective transmittance decreases with increasing sun elevation angles, and with increasing well height. The predictions were about 16% higher than measurements. This difference may be due to the previous assumption in handling a diffuse curb with a specular well combination in SkyVision, and to the reflectance value of the curb and well surfaces, which were not measured.

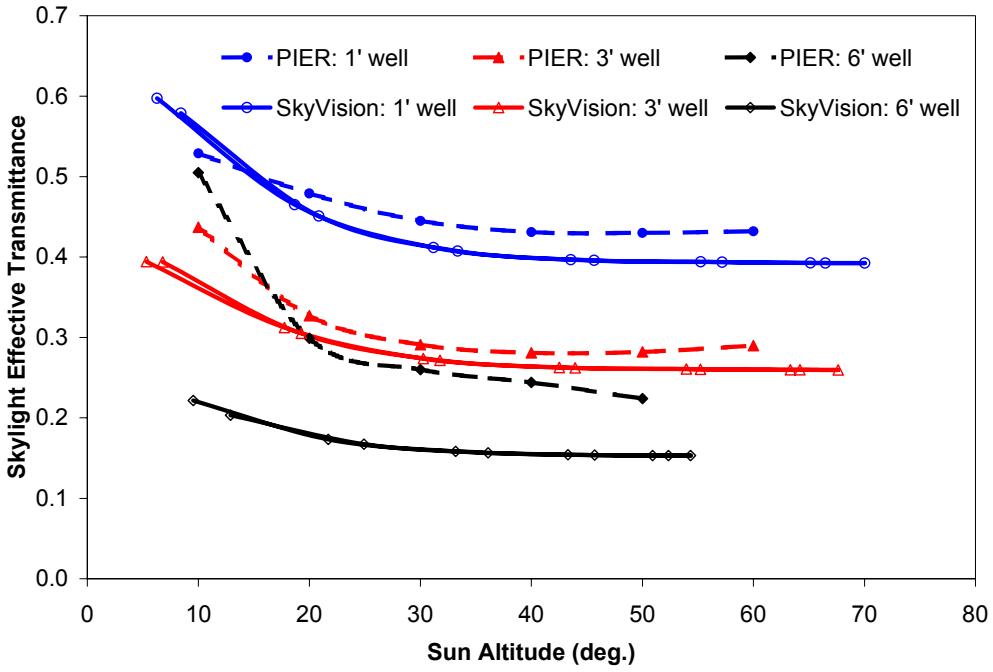

Figure 40 Profile of the skylight effective visible transmittance as a function of the sun's elevation angle – single-glazed diffuse bubble with diffuse well.

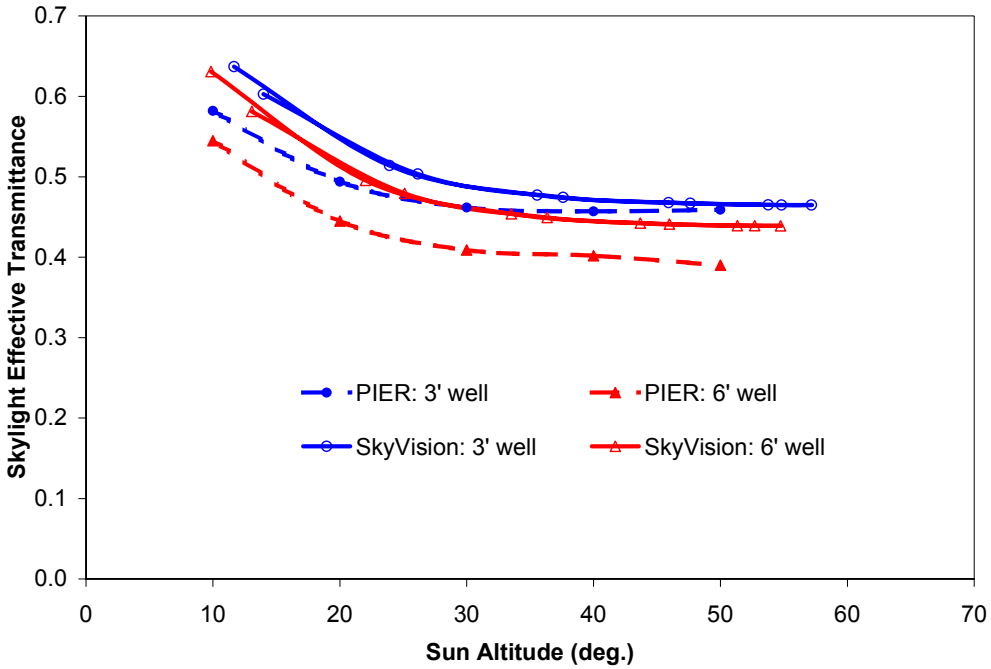

Figure 41 Profile of the skylight effective visible transmittance as a function of the sun's elevation angle – single-glazed diffuse bubble with specular well.

SINGLE CLEAR PYRAMID

Figure 42 shows a comparison between the measured and simulated skylight effective transmittance for the combination of a bronze pyramid and diffuse well. Contrary to the previous results for the diffuse bubble dome, the effective transmittance of the bronze pyramid increases with the sun elevation angles. This trend is typical for transparent nearly-flat skylights. Although the predictions and measurements followed the same trend, the predictions were lower than the measurements by up to 40%, the larger differences occurred at low sun altitude angles. This difference may due to the measurement errors, which were comparable to the low measurement values.

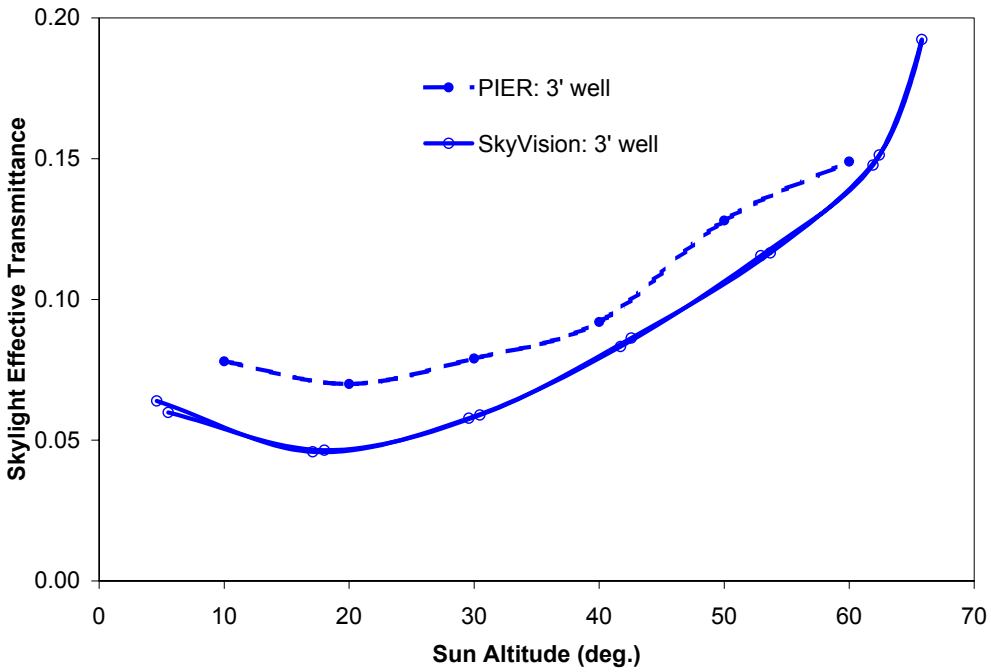

Figure 42 Profile of the skylight effective visible transmittance as a function of the sun's elevation angle – bronze pyramid with diffuse well.

DOUBLE DIFFUSE BUBBLE SKYLIGHT

Figure 43 shows a comparison between the measured and simulated skylight effective transmittance for the combination of a double-glazed diffuse bubble dome and diffuse well. The predictions compared very well with the measurements, particularly for the 3- and 6-foot wells. The maximum deviation between the measurements and predictions occurred for the 1-foot well at low sun altitude angles. This difference may be due to the assumption in the calculation of the glazing transmittance of the dome. As expected, the error involved in this assumption is larger at low sun altitude angles.

Figure 44 shows a comparison between the measured and simulated skylight effective transmittance for the combination of a double-glazed diffuse dome and specular well. Both the predictions and measurements followed the same trend. The effective transmittance decreases with increasing sun elevation angles, and with increasing well height. The difference between predictions and measurements reached 15% for the 6-foot well at high sun altitude angles. This difference may be due to the assumption in handling a diffuse curb with specular well combination in SkyVision, and to the reflectance value of the curb and well surfaces, which were not measured.

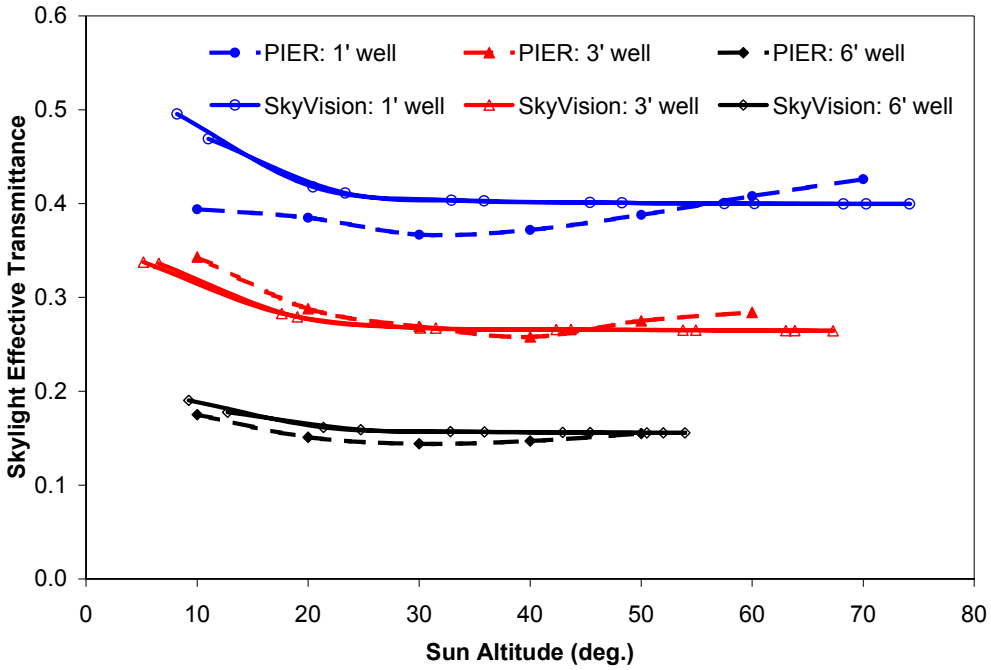

Figure 43 Profile of the skylight effective visible transmittance as a function of the sun's elevation angle – double-glazed diffuse bubble skylight with diffuse well.

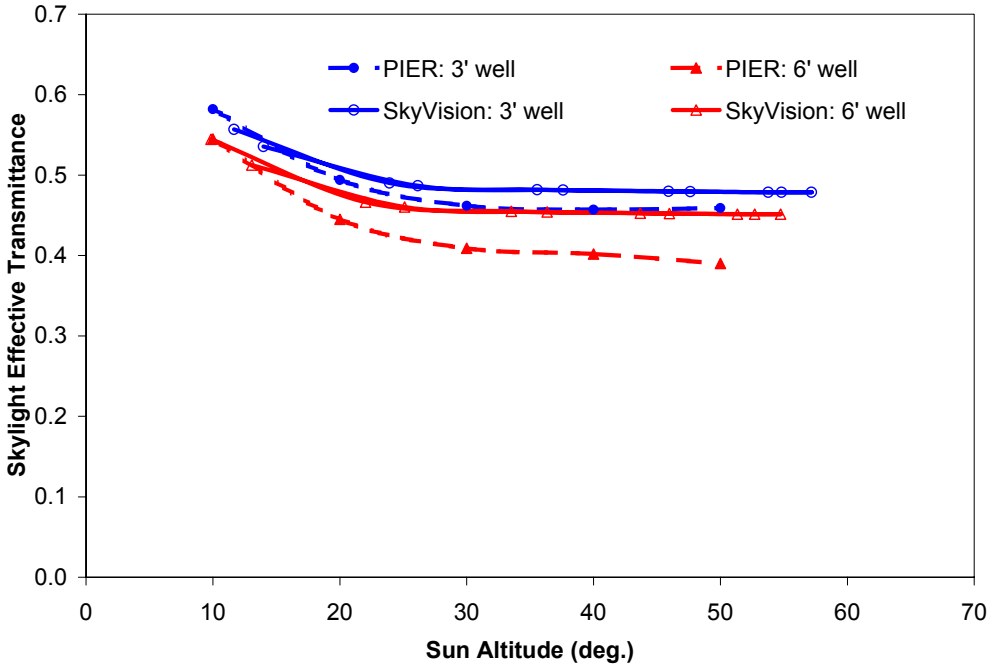

Figure 44 Profile of the effective skylight visible transmittance as a function of the sun's elevation angle – double-glazed diffuse bubble skylight with specular well.

DOUBLE CLEAR FLAT SKYLIGHT

Figure 45 shows a comparison between the measured and simulated skylight effective transmittance for the combination of a double clear low-e flat skylight and diffuse/specular wells. For the diffuse well combination, the predictions were about 20% lower than the measurements, and particularly large at high sun altitude angles. This difference may be due to the effect of the curb and well reflectance values, which were not measured. For the specular well combination, the predictions deviated from the measurements by about 22%. Again, this difference may be due to the previous assumption in handling a diffuse curb with specular well combination in SkyVision, and to the reflectance values of the curb and well surfaces, which were not measured.

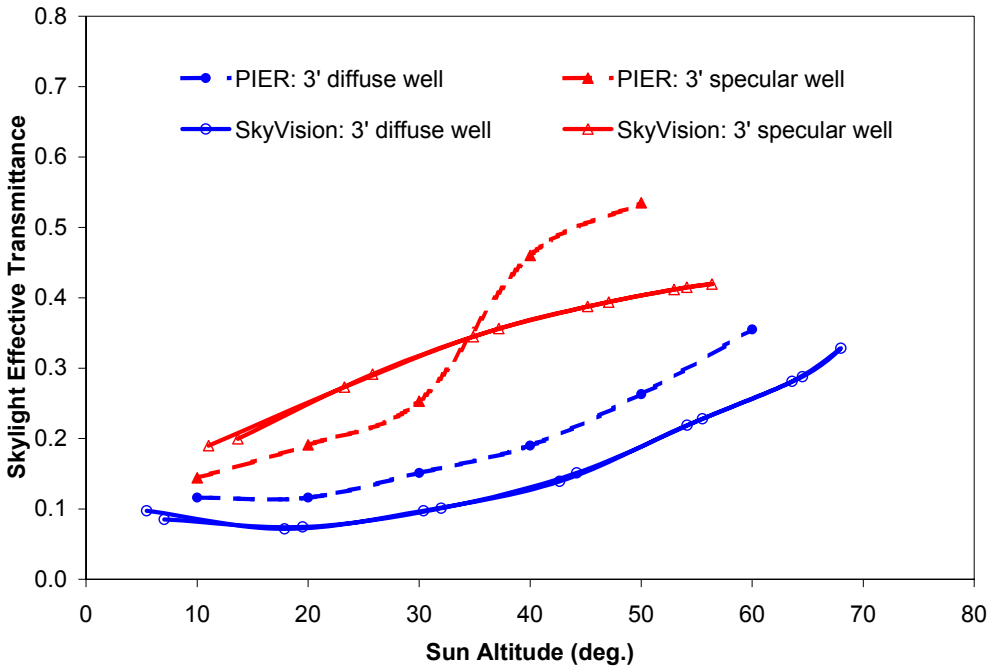

Figure 45 Profile of the skylight effective visible transmittance as a function of the sun's elevation angle – double clear flat skylight with diffuse and specular wells.

CONCLUSIONS

A series of measurements were conducted under real sky conditions to validate the predictions of the SkyVision software. The measurements included the visible transmittance and indoor daylight illuminance of a number of skylight types. The results of the PIER program on the effective transmittance of skylight and well combinations were also used for the validation studies.

When the software's predictions for the skylight transmittance were compared with the actual measurements, they compared very well, except for the hexagonal pyramidal skylight. The predictions

for the hexagonal pyramid were about 30% lower than the measurements, particularly under clear sky conditions. This was due to the fact that the hexagonal pyramid surface exhibited some lens effects around the surface vertices. This effect caused the sensors to measure very low or very high illuminances (under some conditions the interior illuminance sensor readings were about 50% more than the outside illuminance!). The surface lens effect was not possible to model in SkyVision. As for the skylight indoor illuminance comparison, the software's predictions compared very well with the actual measurements for all occurrences of sky conditions.

The software's predictions compared overall well with the results of the skylight effective transmittance measurements of the PIER program, particularly for the skylight and diffuse well combinations. The differences between the predictions and measurements were mainly attributed to the input parameters, which were not measured, and to the limitations of the current version of SkyVision, particularly in handling skylights with a mixture of clear and diffuse glazing, and skylights combined with a diffuse curb and specular well.

RECOMMANDATIONS

The lessons learned from this work suggest the following recommendations:

- Should a similar methodology be adopted to measure the skylight transmittance, an adequate number of illuminance sensors should be used, particularly for skylights with diffuse glazing, or skylights with surface lens effects. The adequate number of sensors is dependent on the skylight size. Sensors should also be adequately placed under the lower part of the skylight surface to capture the transmitted energy by inter-reflection.

- A similar standard to the ASTM Standard E972-96 (or E1084-86/96) should be developed to measure the skylight transmittance under sunlight. Such a standard should be flexible to accommodate typical skylight shapes.

- In practical applications, conventional skylights with lens effects could be used with an additional diffusing glazing pane or with a well diffuser to eliminate/reduce any potential risk of excessive glare and lighting control difficulties.

FUTURE WORK

Future work being considered at this time includes:

- Conducting more experiments to validate other skylight shapes not covered in this report, or in any other related work.

- Enhancing SkyVision to include the calculation of the thermal characteristics of skylights (U-value and SHGC), and prediction of their impact on the heating and cooling energy.

- Developing a rating procedure for skylights.

REFERENCES

1. Brydson J.A., Plastics Materials, 6th edition, Butterworth Heinemann, Oxford, 1995.

2. ASTM Standard E972-96, Standard test method for solar photometric transmittance of sheet materials using sunlight. American Society for Testing and Materials.

3. ASTM Standard E1084-86/96, Standard test method for solar transmittance (terrestrial) of sheet materials using sunlight. American Society for Testing and Materials.

4. CANMET, FRAMEplus 5.1: web site: www.frameplus.net, 2003.

5. Chao B.L., Solatube performance and pay back analysis, International report STI, 1996.

6. HMG, SkyCalc: Skylighting Tool for California and the Pacific Northwest, Heschong Mahone Group: www.h-m-g.com, 2003.

7. IEA SHC Task 21, ADELINE 3.0, RADIANCE and SUPERLITE User's Manual, 2000.

8. Laouadi, A.; Galasiu, A.D.; Atif, M.R.; Haqqani, A. "SkyVision: a software tool to calculate the optical characteristics and daylighting performance of skylights," Building Simulation, 8th IBPSA Conference (Eindhoven, Netherlands, 2003-08-11), pp. 705-712, Aug, 2003a.

9. Laouadi, A.; Galasiu, A.; Atif, M.R. "A New software tool for predicting skylight performance," *International Daylighting,* (5), March, pp. 15-18, Mar, 2003b.

10. Laouadi A., and M.R. Atif, Prediction model of optical characteristics for barrel vault skylights. Journal of the Illuminating Engineering Society of North America, 2002.

11. Laouadi A., and M.R. Atif, Transparent Domed Skylights: Optical Model For Predicting Transmittance, Absorptance And Reflectance, International Journal of Lighting Research and Technology 30(3), pp. 111-118,1998.

12. LBL, WINDOWS 5.1, Lawrence Berkeley Laboratory: http://windows.lbl.gov/, 2003a.

13. LBL, RADIANCE 3.5, Lawrence Berkeley Laboratory: http://radsite.lbl.gov/radiance/, 2003b.

14. Lighting Technologies, Inc., LUMEN MICRO 2000: www.lighting-technologies.com, 2003.

15. McHugh J. Dee R. and Saxena M., Visible Light Transmittance of Skylights, PIER report, California Energy Commission, 2004.

16. Swift P.D. and Smith G.B., Cylindrical mirror light pipes, Solar Energy Material and Solar Cells vol. 36, pp. 159-168, 1995.

17. Zastrow A. and Wittwer V., Daylight with mirror light pipes and with fluorescent planar concentrators, SPIE vol. 692 Materials and optics for solar energy conversion and advanced lighting technology, pp. 227-234, 1986.